π-Stabilized, yet Reactive, Half-Sandwich Cp*Ru(PR$_3$)X Compounds: Synthesis, Structure, and Bonding

Todd J. Johnson,[†] Kirsten Folting,[†] William E. Streib,[†] James D. Martin,[†] John C. Huffman,[†] Sarah A. Jackson,[‡] Odile Eisenstein,*[,‡] and Kenneth G. Caulton*[,†]

Department of Chemistry and Molecular Structure Center, Indiana University, Bloomington, Indiana 47405, and Laboratoire de Chimie Théorique, Bâtiment 490, Université de Paris-Sud, 91405 Orsay, France

Received October 13, 1994[⊗]

The compounds Cp*RuLX (L = P^{i}Pr$_2$Ph, PCy$_3$; X = Cl, Br, I, OCH$_2$CF$_3$, OSiPh$_3$, OSiMe$_2$Ph, NHPh), as well as their CO adducts, have been studied by NMR, IR, and X-ray diffraction in order to understand the nature of the Ru−X bond. Adducts were also formed with C_2H_4. Cp*Ru(P^{i}Pr$_2$Ph)(OCH$_2$CF$_3$) reacts with MeI (but not PhI) to give Cp*Ru(P^{i}Pr$_2$Ph)I and MeOCH$_2$CF$_3$. The compounds Cp*RuLX have a mirror-symmetric structure with Ru, L, X, and the Cp* center coplanar. This is understood, using extended Hückel calculations, to originate in the presence of a Ru−X partial π bond which raises the LUMO. This increases the HOMO−LUMO gap and thus disfavors pyramidalization at the metal center. Calculations of the behavior of systems with X = pure σ donor, π donor, and π acceptor support this analysis. The LUMO of Cp*RuLX still lies low enough to give visible color and to allow rapid addition of (small) Lewis bases. The ν(CO) values of the CO adducts show the X ligand donor power to vary in the order OSiMe$_2$Ph > NHPh > OSiPh$_3$ > OCH$_2$CF$_3$ ≫ Cl > Br > I. Comparison of the Ru−X bond lengthening upon addition of CO is also consistent with this ranking. The lack of facile β-hydrogen migration when X = OCH$_2$CF$_3$ is discussed. Crystallographic data: for Cp*Ru(PCy$_3$)(OSiPh$_3$) at −160 °C, a = 12.131(2) Å, b = 17.563(3) Å, c = 10.703(2) Å, α = 102.59(1)°, β = 110.02(1)°, γ = 75.87(1)° with Z = 2 in space group $P\bar{1}$; for Cp*Ru(PCy$_3$)CO(OSiPh$_3$) at −178 °C, a = 11.331(3) Å, b = 17.840(4) Å, c = 21.813(5) Å, and β = 97.53(1)° with Z = 4 in space group $P2_1/n$; for Cp*RuI(P^{i}Pr$_2$Ph) at −172 °C, a = 8.907(1) Å, b = 15.205(2) Å, c = 17.065(2) Å, and β = 100.62(1)° with Z = 4 in space group $P2_1/n$; for Cp*Ru(PCy$_3$)(OCH$_2$CF$_3$) at −173 °C, a = 12.640(3) Å, b = 14.140(3) Å, c = 17.271(4) Å, and β = 101.79(1)° with Z = 4 in space group $P2_1/c$; for Cp*Ru(PCy$_3$)CO(OCH$_2$CF$_3$) at −172 °C, a = 9.607(2) Å, b = 19.704(3) Å, c = 16.370(3) Å, and β = 96.55(1)° with Z = 4 in space group $P2_1/c$.

Introduction

The overwhelming majority of transition metal polyhydrides, MH$_m$L$_n$ where L is a phosphine or a cyclopentadienyl ligand, are 18-electron species. It is a curious characteristic feature that the introduction of a single halide ligand often serves to enable isolation of an apparently unsaturated (16-valence-electron) product (cf. RuH$_6$L$_2$ *vs* RuH$_3$IL$_2$ and IrH$_5$L$_2$ *vs* IrH$_2$ClL$_2$). If multiple halide introduction is also considered, then the examples become numerous: OsH$_4$L$_3$ *vs* OsCl$_3$L$_3$, ReH$_7$L$_2$ *vs* ReCl$_4$L$_2$, ReH$_5$L$_3$ *vs* ReCl$_3$L$_3$, IrH$_5$L$_2$ *vs* IrCl$_4$L$_2$. While this trend might be due to the electron-withdrawing effect of the introduced halide (X) causing intramolecular redox reorganization (eq 1), that only requires creation of a dihydrogen ligand

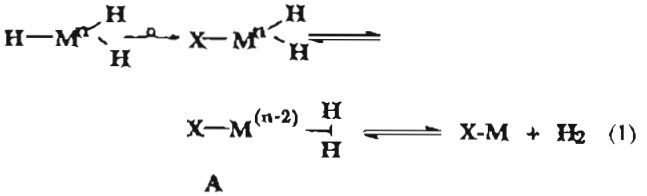

(A) but not its loss from the metal. Indeed, it has been shown that such a species does exist in the form of IrClH$_4$L$_2$, which is IrCl(H)$_2$(H$_2$)L$_2$. This species does however readily lose H$_2$, and thus we are returned to the problem of why unsaturation is a consequence of halide introduction.

Our hypothesis to explain the above trends has been that π donation by halide lone pairs mitigates the unsaturation which is present if the halide were a pure σ-donor ligand.[1] The substructure in **A** suffers a four-electron destabilization between the filled d$_\pi$ orbital and the filled p$_\pi$ orbital on X as shown in **B**.[2] This destabilization can be diminished by the modification

B

of the LUMO and HOMO as the structure at M relaxes in response to H$_2$ dissociation. The loss of H$_2$ thus results from a competition between the coordination of H$_2$ and the partial electron donation from the lone pair of X into the otherwise low-lying LUMO.

This hypothesis is of broad generality (and it has several testable consequences) *beyond* the polyhydride field. The first is that M−X distances should be short in cases conventionally called "unsaturated"[3] and that different X groups should exhibit different degrees of π donation. The second is that incoming donor ligands might be able to overcome this internal compen-

[†] Indiana University.
[‡] Université de Paris-Sud.
[⊗] Abstract published in *Advance ACS Abstracts*, December 15, 1994.

(1) Lunder, D. M.; Lobkovsky, E. B.; Streib, W. E.; Caulton, K. G. *J. Am. Chem. Soc.* **1991**, *113*, 1837.
(2) Poulton, J. T.; Folting, K.; Streib, W. E.; Caulton, K. G. *Inorg. Chem.* **1992**, *31*, 3190.
(3) For an extensive discussion of the meaning(s) of "unsaturated", see: Caulton, K. G. *New J. Chem.* **1994**, *18*, 25.

0020-1669/95/1334-0488$09.00/0

sation (which we will call "π-stabilized unsaturation") and thus exhibit *facile* coordination. The compounds are, therefore, *operationally* unsaturated. Here, we envision the energy profile

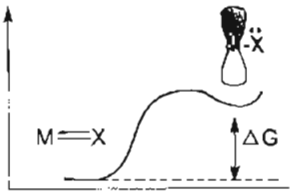

and facile binding results since little or no activation energy is involved in binding a ligand to the purely σ-bonded tautomer. The reshuffling of electrons and the associated geometry changes may either be unimolecular (as shown) or be in response to an incoming donor molecule. The latter (concerted) situation will make ΔG less positive, or even negative since a new bond is formed. Finally, this reasoning suggests[4] that π-stabilized unsaturated compounds may readily bind H_2, and some of these may be dihydrogen compounds (species A in eq 1).

We report here the results of our pursuit of these ideas.

Experimental Section

General Procedures. All manipulations were carried out under an N_2 atmosphere using standard Schlenk techniques. All glassware was flame-dried under vacuum prior to use. Solid transfers were accomplished in a Vacuum Atmospheres Corp. glovebox. Toluene, hexanes, pentane, and diethyl ether were distilled under nitrogen from K/benzophenone and degassed (freeze/pump/thaw) prior to use. C_7D_8 was dried over NaK prior to use and stored in the glovebox. Carbon monoxide (99.8%, Air Products), ^{13}CO (99%, Monsanto), and tricyclohexylphosphine (97%, Aldrich) were used as received without further purification. Cp*Ru(P^{i}Pr$_2$Ph)(Cl) was made by following the procedure for Cp*Ru(PR$_3$)(Cl) [PR$_3$ = PCy$_3$, P^{i}Pr$_3$],[5] P^{i}Pr$_2$Ph,[6] K(O^{i}Pr),[7] K(OSiPh$_3$),[8] K(OSiMe$_2$Ph),[9] and Li(NHPh)[10] were synthesized according to published procedures. The Cp*Ru(P^{i}Pr$_2$Ph)X compounds were sometimes found to be oils, and their composition was therefore determined by mass spectrometry rather than by combustion analysis.

All NMR measurements were made in toluene-d_8, and the ^{1}H, ^{31}P-{^{1}H}, ^{13}C{^{1}H}, and ^{19}F NMR spectra were recorded on a Nicolet NT360 spectrometer at 361.1, 146.2, 90.8, and 339.7 MHz. Positive ^{1}H NMR chemical shifts are downfield of TMS (0.0 ppm). Negative ^{31}P NMR chemical shifts are upfield from external 85% H_3PO_4 (0.0 ppm). All negative ^{19}F chemical shifts are upfield from external CCl_3F (0.0 ppm). IR spectra were recorded on a 510P Nicolet FTIR instrument, as solutions in toluene-d_8. For reactions with gases in an NMR tube, glass tubes fitted with a Teflon valve closure were employed. Desorption chemical ionization (CH_5^-) mass spectrometry (DCI) was used to minimize ligand loss prior to volatilization. Sample temperature was ramped from 250 to 750 °C at 50 °C·s^{-1} and yielded relatively intact monomeric fragments even for the most thermolabile species, Cp*Ru(PCy$_3$)(OCH$_2$CF$_3$).

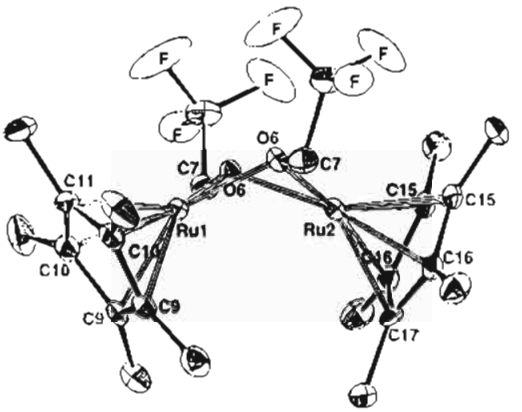

Figure 1. ORTEP drawing of the non-hydrogen atoms of (Cp*RuOCH$_2$CF$_3$)$_2$. A crystallographic mirror plane passes through Ru(1), Ru(2), C(11), and C(17); Ru−O(average) = 2.09 Å.

Syntheses. Tl(OCH$_2$CF$_3$). At 25 °C in a 50 mL flask, 2.9 mL of CF_3CH_2OH (40 mmol) was added to a 20 mL C_6H_6 solution of Tl(OCH$_2$CH$_3$) (1 g, 4 mmol). This solution was stirred for 1 h, and then the excess solvents were distilled away, leaving a yellow oil in the flask. This oil was sublimed (5 mTorr, 75 °C) to yield a crystalline white powder. Yield: 85%. ^{1}H NMR (25 °C): δ 3.71 (q, J_{HF} = 9 Hz, OCH$_2$CF$_3$).

[Cp*Ru(μ_2-OCH$_2$CF$_3$)]$_2$. In a 100 mL flask, a 20 mL pentane solution of Tl(OCH$_2$CF$_3$) (31 mg, 0.10 mmol) was added to a 25 mL pentane slurry of [Cp*Ru(μ_3-Cl)]$_4$ (28 mg, 0.25 mmol). Within 5 min, gray solid had settled out of a cherry red solution. After 1 h, this solution was filtered and stripped to a powder *in vacuo*. A concentrated Et$_2$O solution (3 mL, −20 °C) of this solid yielded red crystals in 80% yield. ^{1}H NMR (25 °C): δ 5.12 (q, J_{HF} = 9 Hz, 2H, OCH$_2$CF$_3$), 1.45 (s, 15H, C$_5$Me$_5$). The solid-state structure of this molecule is shown in Figure 1; see supplementary material for details.

Cp*Ru(P^{i}Pr$_2$Ph)(I). A 10 mL pentane solution of P^{i}Pr$_2$Ph (39 mg, 0.2 mmol) was added to a 20 mL pentane slurry containing [Cp*Ru(μ_3-I)]$_4$[11] (72 mg, 0.05 mmol). The rust-colored slurry immediately gave way to an indigo blue solution. This solution was left overnight at −20 °C. Dark blue crystals were subsequently isolated and dried under vacuum, giving a 75% isolated yield. ^{1}H NMR: δ 7.8 (dd, J_{HH} = 14, 7 Hz, 2H, o-Ph), 7.3−7.0 (m, 3H, m,p-Ph), 2.34 (d of septets, J_{PH} = 10 Hz, J_{HH} = 7 Hz, 2H, CH), 1.23 (s, 15H, C$_5$Me$_5$), 0.95 and 0.88 (each a dd, J_{PH} = 10 Hz, J_{HH} = 7 Hz, 6H, C(CH$_3$)$_2$). ^{31}P NMR: δ 56.2 (s). Anal. Calcd for C$_{22}$H$_{34}$IPRu: C, 47.40; H, 6.15. Found: C, 46.94; H, 6.04.

Cp*Ru(PR$_3$)(X) Complexes. Use of the appropriate phosphine (P^{i}Pr$_2$Ph or PCy$_3$) and [Cp*Ru(μ_3-X)]$_4$ (X = Cl, Br) yields Cp*Ru(PR$_3$)(X) as described for Cp*Ru(P^{i}Pr$_2$Ph)(I). These halide complexes are conveniently synthesized in hexanes, pentane, or diethyl ether. For the other X groups, a 5 mL toluene solution of a given MX salt [1:1 Ru:MX; MX = Tl(OCH$_2$CF$_3$), K(OSiPh$_3$), K(OSiMe$_2$Ph), Li(NHPh)] is added to Cp*Ru(PR$_3$)(Cl) (prepared *in situ*), causing an immediate color change to purple/violet with precipitation of MCl. These solutions were stirred for 15 min and filtered. Solvent was removed *in vacuo* and typically yielded oils for P^{i}Pr$_2$Ph and powders for PCy$_3$. Yields for Cp*Ru(P^{i}Pr$_2$Ph)(X) complexes were found to be quantitative by ^{1}H and ^{31}P NMR.

(a) Cp*Ru(P^{i}Pr$_2$Ph)(Cl). ^{1}H NMR: δ 7.7 (dd, J_{HH} = 14, 7 Hz, 2H, o-Ph), 7.3−7.0 (m, 3H, m,p-Ph), 2.30 (d of septets, J_{PH} = 10 Hz, J_{HH} = 7 Hz, 2H, CH), 1.33 (s, 15H, C$_5$Me$_5$), 0.91 and 0.89 (each a dd, J_{PH} = 12 Hz, J_{HH} = 7 Hz, 6H, C(CH$_3$)$_2$). ^{31}P NMR: δ 49.6(s).

(b) Cp*Ru(P^{i}Pr$_2$Ph)(Br). ^{1}H NMR: δ 7.7 (dd, J_{HH} = 14, 7 Hz, 2H, o-Ph), 7.23−7.09 (m, 3H, m,p-Ph), 2.25 (d of septets, J_{PH} = 10 Hz, J_{HH} = 7 Hz, 2H, CH), 1.29 (s, 15H, C$_5$Me$_5$), 0.93 and 0.88 (each a dd, J_{PH} = 15 Hz, J_{HH} = 7 Hz, 6H, C(CH$_3$)$_2$). ^{31}P NMR: δ 51.8 (s).

(c) Cp*Ru(P^{i}Pr$_2$Ph)(OCH$_2$CF$_3$). ^{1}H NMR: δ 7.7 (dd, J_{HH} = 14, 7 Hz, 2H, o-Ph), 7.3−7.0 (m, 3H, m,p-Ph), 5.08 (q, J_{HF} = 9 Hz, 2H, OCH$_2$CF$_3$), 2.12 (d of septets, J_{PH} = 10 Hz, J_{HH} = 7 Hz, 2H, CH),

(4) Johnson, T. J.; Huffman, J. C.; Caulton, K. G. *J. Am. Chem. Soc.* **1992**, *114*, 2725.

(5) Campion, B. K.; Heyn, R. H.; Tilley, T. D. *J. Chem. Soc., Chem. Commun.* **1988**, 278.

(6) Following the published procedure for PMe$_2$Ph: Adams, D. M.; Raynor, J. R. *Advanced Practical Inorganic Chemistry*; Wiley and Sons, Ltd.: London, 1965; p 116.

(7) Morten, A. A.; Bolton, F. H. *J. Am. Chem. Soc.* **1953**, *75*, 1146. This procedure was slightly modified: We slowly added 1 equiv of HO^{i}Pr to a toluene/KH slurry at 25 °C. The resulting salt was filtered off and dried on a glass frit *in vacuo*.

(8) McGeary, M. J.; Caulton, K. G. *Polyhedron* **1991**, *10*, 2699.

(9) Fuentes, G. R.; Coan, P. S.; Streib, W. E.; Caulton, K. G. *Polyhedron* **1991**, *10*, 2371.

(10) Burdon, J.; Westwood, W. T. *J. Chem. Soc. C* **1970**, 1271. We modified this procedure by reacting *n*-butyllithium and aniline in pentane. The resulting salt was filtered off, washed, and dried on a glass frit.

(11) Fagan, P. J.; Mahoney, W. S.; Calabrese, J. C.; Williams, I. D. *Organometallics* **1990**, *9*, 1843.

1.35 (d, J_{PCp^*} = 1 Hz, 15H, C_5Me_5), 0.94 and 0.93 (each a dd, J_{PH} = 10 Hz, J_{HH} = 7 Hz, 6H, $C(CH_3)_2$). ^{31}P NMR: δ 47.6 (s). ^{19}F NMR: δ −76.8 (t, J_{HF} = 9 Hz). Mass spectrometry (DCI), *m/z*: $Cp^*Ru(P^iPrPh)(OCH_2CF_3)^+$, 487; $Cp^*Ru(P^iPr_2Ph)(OCH_2)^+$, 461; $Cp^*Ru(P^iPr_2Ph)(O)^+$, 447; $Cp^*Ru(PPh)(OCH_2CF_3)^+$, 444; $Cp^*Ru(P^iPr_2Ph)^+$, 431; $Ru(P^iPr_2Ph)(OCH_2CF_3)^+$, 395. Mass spectrometry (CI), *m/z*: $([Cp^*Ru(OCH_2CF_3)]_2 - H)^+$, 671; $[Cp^*Ru]_2^+$, 474.

(d) $Cp^*Ru(PCy_3)(OCH_2CF_3)$. ^1H NMR: δ 5.05 (q, J_{HF} = 9 Hz, 2H, OCH_2CF_3), 2.1−1.2 (m, 33H, C_6H_{11}), 1.48 (s, 15H, C_5Me_5). ^{31}P NMR: δ 37.9 (s). Yield: 85%. Mass spectrometry (DCI): $(Cp^*Ru(PCy_3)(OCH_2CF_3) - H)^+$, 615; $Cp^*Ru(PCy_3)^+$, 517; $Ru(PCy_3)^+$, 382; $Ru(OCH_2CF_3)^+$, 200. Mass spectrometry (CI), *m/z*: $([Cp^*Ru(OCH_2CF_3)]_2 - H)^+$, 671; $[Cp^*Ru]_2^+$, 474.

(e) $Cp^*Ru(P^iPr_2Ph)(OSiPh_3)$. ^1H NMR: δ 7.92 (m, 6H, o-Ph(Si)), 7.63 (m, 2H, o-Ph(P)), 7.28−7.09 (m, 12H, m,p-Ph), 1.91 (d of septets, J_{PH} = 10 Hz, J_{HH} = 7 Hz, 2H, CH), 1.24 (s, 15H, C_5Me_5), 0.85 and 0.81 (each a dd, J_{PH} = 10 Hz, J_{HH} = 7 Hz, 6H, $C(CH_3)_2$). ^{31}P NMR: δ 46.5 (s). Mass spectrometry (CI), *m/z*: $Cp^*Ru(P^iPrPh)(OSiPh_3)^+$, 663; $Cp^*Ru(OSiPh_2)^+$, 435; $Cp^*Ru(P^iPr_2Ph)^+$, 431; $Ru(OSiPh_3)^+$, 377; $Cp^*Ru(OSiPh)^+$, 358.

(f) $Cp^*Ru(PCy_3)(OSiPh_3)$. ^1H NMR: δ 7.98 (dd, J_{HH} = 14, 7 Hz, 6H, o-Ph), 7.30 (dd, J_{HH} = 14, 7 Hz, 6H, m-Ph), 7.27 (dd, J_{HH} = 14, 7 Hz, 3H, p-Ph), 2.0−1.0 (m, 33H, C_6H_{11}), 1.34 (s, 15H, C_5Me_5). ^{31}P NMR: δ 39.4 (s). Yield: 91%. Mass spectrometry (CI), *m/z*: $Cp^*Ru(PCy_3)(OSiPh_3)^+$, 715; $Ru(PCy_3)(OSiPh_3)^+$, 657; $Cp^*Ru(PCy_3)(OSiPh_2)^+$, 638; $Cp^*Ru(PCy_3)^+$, 517; $Cp^*Ru(OSiPh_3)^+$, 512; $Ru(OSiPh_3)^+$, 377.

(g) $Cp^*Ru(P^iPr_2Ph)(OSiMe_2Ph)$. ^1H NMR: δ 8.0−7.0 (m, 10H, Ph), 2.02 (d of septets, J_{PH} = 10 Hz, J_{HH} = 7 Hz, 2H, CH), 1.34 (s, 15H, C_5Me_5), 0.88 and 0.87 (each a dd, J_{PH} = 11 Hz, J_{HH} = 7 Hz, 6H, $C(CH_3)_2$), 0.55 (s, 6H, $Si(CH_3)_2$). ^{31}P NMR: δ 47.1 (s).

(h) $Cp^*Ru(P^iPr_2Ph)(NHPh)$. ^1H NMR: δ 7.46−6.63 (m, 10H, Ph), 2.39 (d of septets, J_{PH} = 10 Hz, J_{HH} = 7 Hz, 2H, CH), 1.62 (s, 15H, C_5Me_5), 1.13 and 0.82 (each a dd, J_{PH} = 12 Hz, J_{HH} = 7 Hz, 6H, $C(CH_3)_2$). ^{31}P NMR: δ 58.9 (s).

Synthesis of $Cp^*Ru(PR_3)(X)(CO)$ Complexes. Typically, 0.2 mmol of $Cp^*Ru(PR_3)(X)$ was dissolved in 10 mL of Et_2O. This solution was exposed to 3.0 mmol of CO at 1 atm, causing an immediate color change to orange/yellow. After 2 min (25 °C), the solution was concentrated in vacuo to *ca.* 3.0 mL and was placed in a −20 °C freezer. Crystallization of $Cp^*Ru(PR_3)(X)(CO)$ usually occurred within 48 h.

(a) $Cp^*Ru(P^iPr_2Ph)(I)(CO)$. ^1H NMR: δ 7.68 (dd, J_{HH} = 14, 7 Hz, 2H, o-Ph), 7.07−7.01 (m, 3H, m,p-Ph), 3.45 and 2.20 (each a d of septets, J_{PH} = 10 Hz, J_{HH} = 7 Hz, 1H, CH), 1.45 (d, J_{PCp^*} = 1.3 Hz, 15H, C_5Me_5), 1.41, 1.21, 1.16, and 0.83 (each a dd, J_{PH} = 15 Hz, J_{HH} = 7 Hz, 3H, $C(CH)_3)_2$). ^{31}P NMR: δ 54.6 (s). ^{13}C NMR: δ 209.2 (d, J_{PC} = 18 Hz). ν_{CO} = 1930 cm^{-1}. Yield: 80%.

(b) $Cp^*Ru(P^iPr_2Ph)(Br)(CO)$. ^1H NMR: δ 7.7 (dd, J_{HH} = 14, 7 Hz, 2H, o-Ph), 7.12−7.09 (m, 3H, m,p-Ph), 3.28 and 2.25 (each a d of septets, J_{PH} = 10 Hz, J_{HH} = 7 Hz, 1H, CH), 1.48, 1.18, 1.12, and 0.84 (each a dd, J_{PH} = 16−12 Hz, J_{HH} = 7 Hz, 3H, $C(CH_3)_2$), 1.38 (d, J_{PCp^*} = 1.4 Hz, 15H, C_5Me_5). ^{31}P NMR: δ 54.7 (s). ν_{CO} = 1928 cm^{-1}. Yield: 80%.

(c) $Cp^*Ru(P^iPr_2Ph)(Cl)(CO)$. ^1H NMR: δ 7.69 (dd, J_{HH} = 14, 7 Hz, 2H, o-Ph), 7.12−7.04 (m, 3H, m,p-Ph), 3.13 and 2.24 (each of d of septets, J_{PH} = 10 Hz, J_{HH} = 7 Hz, 1H, CH), 1.34 (d, J_{PCp^*} = 1.5 Hz, 15H, C_5Me_5), 1.51, 1.19, 1.06, and 0.84 (each a dd, J_{PH} = 16−12 Hz, J_{HH} = 7 Hz, 3H, $C(CH_3)_2$). ^{31}P NMR: δ 55.3 (s). ^{13}C NMR: δ 208.9 (d, J_{PC} = 19 Hz). ν_{CO} = 1925 cm^{-1}. Yield: 84%.

(d) $Cp^*Ru(P^iPr_2Ph)(OCH_2CF_3)(CO)$. ^1H NMR: δ 7.95 (dd, J_{HH} = 14, 7 Hz, 2H, o-Ph), 7.15−7.0 (m, 3H, m,p-Ph), 4.17 and 4.10 (each a dq, J_{HH} = 10 Hz, J_{HF} = 9 Hz, 1H, OCH_2CF_3), 3.27 and 2.16 (each a d of septets, J_{PH} = 10 Hz, J_{HH} = 7 Hz, 1H, CH), 1.31 (d, J_{PCp^*} = 1.6 Hz, 15H, C_5Me_5), 1.49, 1.23, 1.22, and 0.93 (each a dd, J_{PH} = 17−12 Hz, J_{HH} = 7 Hz, 3H, $C(CH_3)_2$). ^{31}P NMR: δ 52.3 (s). ^{13}C NMR: δ 210.4 (d, J_{PC} = 20 Hz). ^{19}F NMR: δ −77.1 (t, J_{HF} = 9 Hz, OCH_2CF_3). ν_{CO} = 1914 cm^{-1}. Yield: 86%.

(e) $Cp^*Ru(PCy_3)(OCH_2CF_3)(CO)$. ^1H NMR: δ 3.99 and 3.93 (each a dq, J_{HH} = 10 Hz, J_{HF} = 9 Hz, 1H, OCH_2CF_3), 2.15−1.80 (m, 33H, C_6H_{11}), 1.59 (d, J_{PCp^*} = 1.3 Hz, 15H, C_5Me_5). ^{31}P NMR: δ 48.6 (s). ν_{CO}: 1909 cm^{-1}. Anal. Calcd for $C_{31}H_{50}F_3O_2PRu$: C, 57.84; H, 7.83. Found: C, 57.65; H, 8.06. Yield: 90%.

(f) $Cp^*Ru(P^iPr_2Ph)(OSiPh_3)(CO)$. ^1H NMR: δ 7.99 (m, 6H, o-Ph-(Si)), 7.65 (m, 2H, o-Ph(P)), 7.3−7.1 (m, 12H, m,p-Ph), 3.10 and 2.11 (each a d of septets, J_{PH} = 10 Hz, J_{HH} = 7 Hz, 1H, CH), 1.20, 0.90, 0.86, and 0.67 (each a dd, J_{PH} = 16−11 Hz, J_{HH} = 7 Hz, 3H, $C(CH_3)_2$), 1.15 (d, J_{PCp^*} = 0.8 Hz, 15H, C_5Me_5). ^{31}P NMR: δ 52.0 (s). ν_{CO} = 1906 cm^{-1}. Yield: 89%.

(g) $Cp^*Ru(PCy_3)(OSiPh_3)(CO)$. ^1H NMR: δ 7.93 (dd, J_{HH} = 14, 7 Hz, 6H, o-Ph), 7.28 (dd, J_{HH} = 14, 7 Hz, 6H, m-Ph), 7.19 (dd, J_{HH} = 14, 7 Hz, 3H, p-Ph), 2.30−0.90 (m, 33H, C_6H_{11}), 1.46 (d, J_{PCp^*} = 1.5 Hz, 15H, C_5Me_5). ^{31}P NMR: δ 50.1 (s). ^{13}C NMR: δ 209.9 (d, J_{PC} = 23 Hz). ν_{CO} = 1902 cm^{-1}. Anal. Calcd for $C_{47}H_{63}O_2SiPRu$: C, 68.83; H, 7.74. Found: C, 69.13; H, 7.65. Yield: 92%.

(h) $Cp^*Ru(P^iPr_2Ph)(OSiMe_2Ph)(CO)$. ^1H NMR: δ 7.9 (m, 2H, o-Ph(Si)), 7.52 (m, 2H, o-Ph(P)), 7.35−7.10 (m, 6H, m,p-Ph), 3.10 and 2.05 (each a d of septets, J_{PH} = 10 Hz, J_{HH} = 7 Hz, 1H, CH), 1.29, 1.21, 1.19, and 0.68 (each a dd, J_{PH} = 15−11 Hz, J_{HH} = 7 Hz, 3H, $C(CH_3)_2$), 1.23 (d, J_{PCp^*} = 1.4 Hz, 15H, C_5Me_5), 0.53 and 0.52 (s, 3H, $SiCH_3$). ^{31}P NMR: δ 51.7 (s). ν_{CO} = 1903 cm^{-1}. Yield: 74%.

(i) $Cp^*Ru(P^iPr_2Ph)(NHPh)(CO)$. ^1H NMR: δ 7.46−6.36 (m, 10H, Ph), 2.50 and 2.24 (each a d of septets, J_{PH} = 10 Hz, J_{HH} = 7 Hz, 1H, CH), 1.40 (d, J_{PCp^*} = 1.4 Hz, 15H, C_5Me_5), 1.16, 1.06, 1.01, and 0.92 (each a dd, J_{PH} = 15−12 Hz, J_{HH} = 7 Hz, 3H, $C(CH_3)_2$). ^{31}P NMR: δ 56.1 (s). ν_{CO} = 1904 cm^{-1}. Yield: 72%.

NMR Tube Reactions of $Cp^*Ru(P^iPr_2Ph)(X)$ with C_2H_4. An NMR tube containing a frozen (−196 °C) toluene-d_8 solution of $Cp^*Ru(P^iPr_2Ph)(X)$ (X = Cl, I, OR_f; 0.10 mmol) was exposed to 0.10 mmol of $^{13}C_2H_4$ (99%); the tube was sealed after the ethylene gas had condensed.

(a) $Cp^*Ru(P^iPr_2Ph)(C_2H_4)(Cl)$. $^{31}P\{^1H\}$ NMR (−60 °C): δ 56.0 (s). $^{13}C\{^1H\}$ NMR (−60 °C): δ 49.9 and 39.8 (each a d, J_{CC} = 44 Hz).

(b) $Cp^*Ru(P^iPr_2Ph)(C_2H_4)(I)$. $^{31}P\{^1H\}$ NMR (−60 °C): δ 56.6 (s). $^{13}C\{^1H\}$ NMR (−60 °C): δ 42.7 and 39.6 (each a d, J_{CC} = 44 Hz).

(c) $Cp^*Ru(P^iPr_2Ph)(C_2H_4)(OCH_2CF_3)$. $^{31}P\{^1H\}$ NMR (−60 °C): δ 56.1 (s). $^{13}C\{^1H\}$ NMR (−60 °C): δ 40.9 and 40.4 (each a d, J_{CC} = 44 Hz).

Reaction of $Cp^*Ru(P^iPr_2Ph)(OCH_2CF_3)$ with MeI. At room temperature, methyl iodide (1.0 mL, 16 mmol) was added to a 100 mL Schlenk flask containing 25 mL of a pentane solution of $Cp^*Ru(P^iPr_2Ph)(OCH_2CF_3)$ (0.1 mmol). This reaction was stirred for 1 h. Volatiles were then removed *in vacuo*. The resulting blue oil was dissolved in 5 mL of pentane, and the solution was cooled to −20 °C. After 24 h at this temperature, dark blue crystals formed. These were isolated and shown to be $Cp^*Ru(P^iPr_2Ph)(I)$ by ^1H and ^{31}P NMR spectroscopy.

Interaction of $Cp^*Ru(P^iPr_2Ph)(OCH_3CF_3)$ with Chlorobenzene. Chlorobenzene (30 μL, 0.3 mmol) was added to an NMR tube containing 0.5 mL of a toluene-d_8 solution of $Cp^*Ru(P^iPr_2Ph)(OCH_2CF_3)$ (0.1 mmol) at 25 °C. At this temperature, ^1H and ^{31}P NMR showed no interaction between these molecules. The NMR spectra of these nuclei were invariant from +25 to −60 °C.

Structure Determination of $Cp^*RuI(P^iPr_2Ph)$. A crystal of suitable size was mounted in a nitrogen atmosphere glovebag using silicone grease, and it was then transferred to a goniostat where it was cooled to −172 °C for characterization and data collection (Table 1).[12] A search of a limited hemisphere of reciprocal space revealed intensities with Laue symmetry and systematic absences consistent with space group $P2_1/n$, which was later confirmed by the successful solution of the structure. Following complete data collection ($6° < 2\theta < 45°$) and correction for absorption, data processing gave a residual of 0.027 for the averaging of 1231 unique intensities which had been observed more than once. Four standards measured every 300 data showed no significant trends. The structure was solved using a combination of direct methods (MULTAN78) and Fourier techniques. The Ru and I positions were determined from an *E* map. The remaining atoms including the hydrogens were obtained from subsequent iterations of least-squares refinement and difference Fourier calculation. In the final

(12) For general instrumental, computer program, and data handling methods, see: Huffman, J. C.; Lewis, L. N.; Caulton, K. G. *Inorg. Chem.* **1980**, *19*, 2755.

Table 1. Crystallographic Data

	Cp*RuI(P^{i}Pr$_2$Ph)	Cp*Ru(PCy$_3$)(OCH$_2$CF$_3$)	Cp*Ru(OCH$_2$CF$_3$)(CO)(PCy$_3$)	Cp*Ru(PCy$_3$)(OSiPh$_3$)	Cp*Ru(PCy$_3$)CO(OSiPh$_3$)
chem formula	$C_{22}H_{34}IPRu$	$C_{30}H_{50}PF_3ORu$	$C_{31}H_{50}F_3O_2PRu$	$C_{46}H_{63}OPSiRu$	$C_{47}H_{63}O_2PRuSi$
a, Å	8.907(1)	12.640(3)	9.607(2)	12.131(2)	11.331(3)
b, Å	15.205(2)	14.140(3)	19.704(3)	17.563(3)	17.840(4)
c, Å	17.065(2)	17.271(4)	16.370(3)	10.703(2)	21.813(5)
α, deg				102.59(1)	
β, deg	100.62(1)	101.79(1)	96.55(1)	110.02(1)	97.53(1)
γ, deg				75.87(1)	
V, Å^3	2271.55	3021.76	3078.64	2054.92	4371.55
Z	4	4	4	2	4
fw	557.46	615.76	643.77	792.13	820.14
space group	$P2_1/n$	$P2_1/c$	$P2_1/c$	$P\bar{1}$	$P2_1/n$
T, °C	−172	−173	−172	−160	−178
λ, Å	0.710 69	0.710 69	0.710 69	0.710 69	0.710 69
ϱ_{calcd}, g cm^{-3}	1.630	1.354	1.389	1.280	1.246
μ (Mo Kα), cm^{-1}	20.95	6.0	5.9	4.7	4.475
R^a	0.0245	0.0699	0.0354	0.0254	0.0419
$R_w{}^b$	0.0279	0.0673	0.0350	0.0296	0.0471

^{a} $R = \sum||F_o| - |F_c||/\sum|F_o|$. ^{b} $R_w = [\sum w(|F_o| - |F_c|)^2/\sum w|F_o|^2]^{1/2}$ where $w = 1/\sigma^2(|F_o|)$.

Table 2. Selected Bond Distances (Å) and Angles (deg) for Cp*RuI(P^{i}Pr$_2$Ph)

I(2)−Ru(1)	2.6642(5)	Ru(1)−C(20)	2.164(4)
Ru(1)−P(3)	2.3773(12)	C(16)−C(17)	1.431(6)
Ru(1)−C(16)	2.142(4)	C(16)−C(20)	1.445(6)
Ru(1)−C(17)	2.181(4)	C(17)−C(18)	1.436(6)
Ru(1)−C(18)	2.139(4)	C(18)−C(19)	1.450(6)
Ru(1)−C(19)	2.174(4)	C(19)−C(20)	1.420(6)
I(2)−Ru(1)−P(3)	94.90(3)	Ru(1)−P(3)−C(7)	114.72(15)
Ru(1)−P(3)−C(4)	113.23(15)	Ru(1)−P(3)−C(10)	117.67(15)

cycles of refinement, the non-hydrogen atoms were varied with anisotropic thermal parameters and the hydrogen atoms were varied with isotropic thermal parameters. The final difference map was essentially featureless, the largest residual peak being 0.54 e/Å^3. The results of the structure determination are shown in Table 2 and Figure 2. Carbon/hydrogen distances range from 0.80(5) to 1.06(6) Å.

Structure Determination of Cp*Ru(PCy$_3$)(OCH$_2$CF$_3$). A suitable single crystal was selected and manipulated in an inert nitrogen atmosphere. The selected crystal was affixed to the end of a glass fiber and transferred to the goniostat where it was cooled to 100 K for characterization and data collection ($6° < 2\theta < 45°$). A search of a limited hemisphere of reciprocal space located a set of diffraction maxima with symmetry and systematic absences corresponding the unique monoclinic space group $P2_1/c$. Subsequent solution and refinement (Table 1) confirmed this choice. No absorption correction was attempted due to the irregular shape of the fragment. Data were collected using a moving crystal/moving detector technique with fixed backgrounds at each extreme of the scan. After correction for Lorentz and polarization terms, a set of unique intensities were generated. The Ru atom was located in a map phased by direct methods (MULTAN78), and two subsequent Fourier maps were able to locate the remaining non-hydrogen atoms. About half of the hydrogen atoms were visible in a difference Fourier map phased on the non-hydrogen atoms. For the final cycles, all hydrogen atoms were placed in fixed idealized positions. A final difference Fourier map was featureless. The results of the structure determination are shown in Table 3 and Figure 3.

Structure Determination of Cp*Ru(PCy$_3$)(OSiPh$_3$). A triangular fragment was cleaved from a dark purple crystal and affixed to the end of a glass fiber using silicone grease. The crystal was then transferred to the goniostat where it was cooled to −160 °C for characterization (Table 1) and data collection ($6° < 2\theta < 45°$). All sample handling employed standard inert atmosphere techniques. A systematic search of a limited hemisphere of reciprocal space located no symmetry or systematic absences, indicating a triclinic space group. Subsequent solution and refinement confirmed the centrosymmetric $P\bar{1}$. Data were collected using a $\theta-2\theta$ scan with fixed backgrounds at each extreme of the scan. Equivalent data were averaged after being corrected for Lorentz and polarization terms. The Ru atom was located using direct methods (MULTAN78), and the remaining atoms were readily located using Fourier techniques. Hydrogen atoms were visible in a difference Fourier map phased on the refined non-hydrogen atoms and were refined isotropically in the final cycles. A final difference Fourier map was featureless, the largest peak being 0.36 e/Å^3. The results of the structure determination are shown in Table 4 and Figure 4.

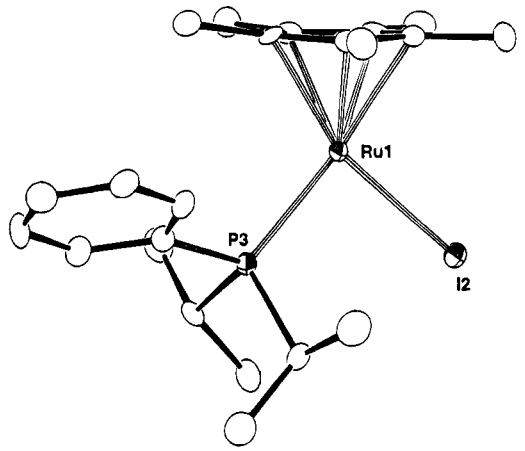

Figure 2. ORTEP drawing of the non-hydrogen atoms of Cp*Ru(P^{i}Pr$_2$Ph)I showing selected atom labeling.

Table 3. Selected Bond Distances (Å) and Angles (deg) for Cp*Ru(PCy$_3$)(OCH$_2$CF$_3$)

Ru(1)−P(18)	2.418(4)	F(5)−C(4)	1.367(18)
Ru(1)−O(2)	1.992(10)	F(6)−C(4)	1.339(18)
Ru(1)−C(8)	2.159(14)	F(7)−C(4)	1.315(20)
Ru(1)−C(9)	2.175(17)	O(2)−C(3)	1.357(19)
Ru(1)−C(10)	2.155(14)	C(3)−C(4)	1.511(23)
Ru(1)−C(11)	2.140(13)	C(8)−C(9)	1.378(21)
Ru(1)−C(12)	2.165(12)	C(8)−C(12)	1.480(20)
P(18)−C(19)	1.859(17)	C(9)−C(10)	1.422(23)
P(18)−C(25)	1.862(15)	C(10)−C(11)	1.449(20)
P(18)−C(31)	1.850(16)	C(11)−C(12)	1.359(20)
P(18)−Ru(1)−O(2)	81.6(3)	O(2)−C(3)−C(4)	109.0(13)
Ru(1)−P(18)−C(19)	119.9(5)	F(5)−C(4)−F(6)	103.7(12)
Ru(1)−P(18)−C(25)	109.4(5)	F(5)−C(4)−F(7)	106.6(15)
Ru(1)−P(18)−C(31)	112.3(5)	F(5)−C(4)−C(3)	112.1(14)
C(19)−P(18)−C(25)	109.4(7)	F(6)−C(4)−F(7)	106.1(15)
C(19)−P(18)−C(31)	102.5(7)	F(6)−C(4)−C(3)	112.5(15)
Ru(1)−O(2)−C(3)	124.6(9)	F(7)−C(4)−C(3)	115.1(13)

Structure Determination of Cp*Ru(OCH$_2$CF$_3$)(CO)(PCy$_3$). A rodlike crystal was obtained by cleaving a cluster of crystals in a nitrogen atmosphere glove bag. The crystal was mounted using silicone grease and was then transferred to a goniostat where it was cooled to −172 °C for characterization and data collection (Table 1). A search of a limited hemisphere of reciprocal space revealed intensities with Laue symmetry and systematic absences consistent with space group

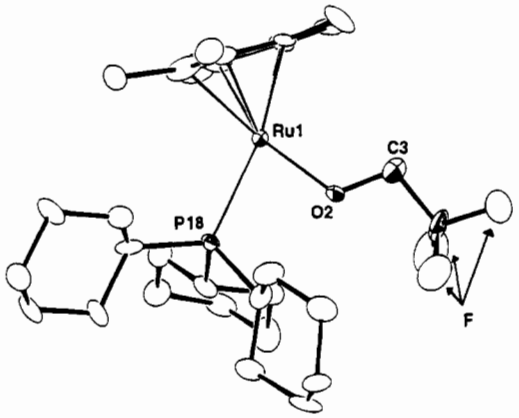

Figure 3. ORTEP drawing of the non-hydrogen atoms of Cp*Ru(PCy$_3$)(OCH$_2$CF$_3$) showing selected atom labeling.

Table 4. Selected Bond Distances (Å) and Angles (deg) for Cp*Ru(PCy$_3$)(OSiPh$_3$)

Ru(1)−P(32)	2.3961(7)	Si(13)−O(12)	1.5908(18)
Ru(1)−O(12)	2.0278(17)	Si(13)−C(14)	1.8828(26)
Ru(1)−C(2)	2.1519(24)	Si(13)−C(20)	1.8890(26)
Ru(1)−C(3)	2.1705(24)	Si(13)−C(26)	1.8883(25)
Ru(1)−C(4)	2.1183(23)	C(2)−C(3)	1.414(4)
Ru(1)−C(5)	2.1678(24)	C(2)−C(6)	1.438(4)
Ru(1)−C(6)	2.1523(24)	C(3)−C(4)	1.448(4)
P(32)−C(33)	1.8554(25)	C(4)−C(5)	1.439(4)
P(32)−C(39)	1.8489(25)	C(5)−C(6)	1.422(4)
P(32)−O(12)	1.5908(18)		

P(32)−Ru(1)−O(12)	85.01(5)	C(14)−Si(13)−C(20)	107.79(12)
Ru(1)−P(32)−C(33)	116.24(9)	C(14)−Si(13)−C(26)	105.60(11)
Ru(1)−P(32)−C(39)	107.75(8)	C(20)−Si(13)−C(26)	107.01(11)
Ru(1)−P(32)−C(45)	117.46(8)	Ru(1)−O(12)−Si(13)	153.49(11)
C(33)−P(32)−C(39)	103.19(11)	Si(13)−C(14)−C(15)	121.42(20)
C(33)−P(32)−C(45)	101.33(11)	Si(13)−C(14)−C(19)	121.38(20)
C(39)−P(32)−C(45)	109.87(12)	Si(13)−C(20)−C(21)	119.83(21)
O(12)−Si(13)−C(14)	111.44(10)	Si(13)−C(20)−C(25)	123.13(22)
O(12)−Si(13)−C(20)	114.21(11)	Si(13)−C(26)−C(27)	124.60(19)
O(12)−Si(13)−C(26)	110.34(10)	Si(13)−C(26)−C(31)	118.76(19)

$P2_1/c$ which was later confirmed by the successful solution of the structure. Following complete intensity data collection ($6° < 2\theta < 45°$), data processing gave a residual of 0.030 for the averaging of 1887 unique intensities which had been observed more than once. Four standards measured every 400 data showed no significant trends. No correction was made for absorption. The structure was solved using a combination of direct methods (MULTAN78) and Fourier techniques. The Ru and P positions were determined from an initial E map. The remaining atoms were obtained from subsequent iterations of least-squares refinement and difference Fourier calculation. Almost all of the hydrogens were observed in the difference maps, and all were placed in calculated positions prior to refinement. In the final cycles of refinement, the non-hydrogen atoms were varied with anisotropic thermal parameters. The final difference map was essentially featureless, the largest peak being 0.55 e/Å^3. The results of the structure determination are shown in Table 5 and Figure 5.

Structure Determination of Cp*Ru(PCy$_3$)(CO)(OSiPh$_3$). A fragment was cleaved from a large crystal (>2 mm) and was affixed to the end of a glass fiber with silicone grease and transferred to the goniostat where it was cooled to −178 °C for characterization (Table 1) and data collection ($6° < 2\theta < 45°$). Standard inert atmosphere techniques were employed. A systematic search of a limited hemisphere of reciprocal space yielded a set of reflections which exhibited monoclinic symmetry. The systematic extinction of $0k0$ for $k = 2n + 1$ and of $h0l$ for $h + l = 2n + 1$ uniquely identified the space group as $P2_1/n$. The structure was solved using MULTAN and standard Fourier techniques. The Ru and P atoms were located in the initial E map, and the remainder of the non-hydrogen atoms were located by successive difference Fourier maps. Almost all of the Cp methyl hydrogens were located in the difference map; all other hydrogens were placed in calculated positions. All hydrogen positions were fixed in the final least-squares refinement. In addition to the ruthenium complex, a disordered hydrocarbon solvent molecule was located near a center of symmetry. Only two atoms, C(53) and C(54), of these molecules were located and used in the final refinement. The shortest contact between this fragment and the ruthenium complex is 3.6 Å. The full-matrix least-squares refinement was completed using anisotropic thermal parameters on all non-hydrogen atoms and isotropic thermal parameters on the hydrogen atoms. The final difference map was essentially featureless except for several peaks, the largest of which exhibited 1.5 e/Å^3, located in the immediate vicinity of the disordered solvent. Results are shown in Table 6 and Figure 6.

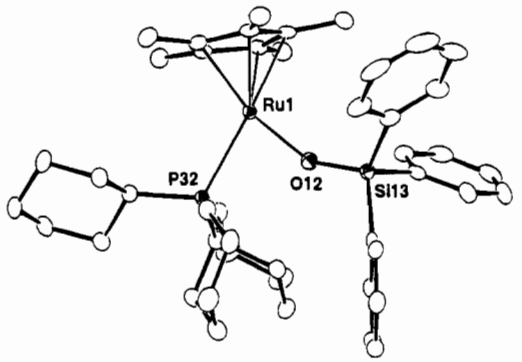

Figure 4. Drawing of Cp*Ru(PCy$_3$)(OSiPh$_3$) viewed nearly perpendicular to the idealized mirror plane. The bend at O(12) occurs almost entirely in the plane of the paper.

Table 5. Selected Bond Distances (Å) and Angles (deg) for Cp*Ru(OCH$_2$CF$_3$)(CO)(PCy$_3$)

Ru(1)−P(2)	2.3761(12)	F(24)−C(23)	1.335(5)
Ru(1)−O(21)	2.090(3)	F(25)−C(23)	1.334(6)
Ru(1)−C(27)	1.833(4)	F(26)−C(23)	1.350(5)
Ru(1)−C(29)	2.329(4)	O(21)−C(22)	1.357(6)
Ru(1)−C(30)	2.296(4)	O(28)−C(27)	1.163(5)
Ru(1)−C(31)	2.232(4)	C(22)−C(23)	1.502(7)
Ru(1)−C(32)	2.215(4)	C(29)−C(30)	1.404(6)
Ru(1)−C(33)	2.238(4)	C(29)−C(33)	1.458(6)
P(2)−C(3)	1.882(5)	C(30)−C(31)	1.453(6)
P(2)−C(9)	1.850(4)	C(31)−C(32)	1.426(6)
P(2)−C(15)	1.866(4)	C(32)−C(33)	1.419(6)

P(2)−Ru(1)−O(21)	78.78(9)	Ru(1)−O(21)−C(22)	122.94(27)
P(2)−Ru(1)−C(27)	90.96(14)	O(21)−C(22)−C(23)	108.8(4)
O(21)−Ru(1)−C(27)	101.08(16)	F(24)−C(23)−F(25)	106.3(4)
Ru(1)−P(2)−C(3)	115.87(14)	F(24)−C(23)−F(26)	105.6(4)
Ru(1)−P(2)−C(9)	117.61(16)	F(24)−C(23)−C(22)	112.6(4)
Ru(1)−P(2)−C(15)	110.60(14)	F(25)−C(23−F(26)	106.1(4)
C(3)−P(2)−C(9)	103.91(19)	F(25)−C(23)−C(22)	113.2(4)
C(3)−P(2)−C(15)	103.68(20)	F(26)−C(23)−C(22)	112.4(4)
C(9)−P(2)−C(15)	103.61(20)	Ru(1)−C(27)−O(28)	171.9(4)

Computational Details. EHT calculations were carried out using the weighted H_{ij} formula.[13a] The atomic parameters for Ru were taken from the literature.[13b] For all the complexes studied, the following angles and distances were used: Cp(center)−Ru = 1.78 Å, C−C = 1.436 Å; then for CpRuH$_2^-$, Cp(center)−Ru−H = 127.67° and Ru−H = 1.64 Å; for CpRu(PH$_3$)I, Ru−P = 2.379 Å, Ru−I = 2.665 Å, Cp(center)−Ru−P = 138.798°, and Cp(center)−Ru−I = 127.71°; for CpRu(CO)$_2^+$, Ru−C = 2.05 Å, C−O = 1.14 Å, and Cp(center)−Ru−C = 127.6°. The bending motion was carried out using two different orientations of the Cp ring, with the plane L−Ru−X (at $\theta = 180°$) parallel or perpendicular to one of the Cp C−C bonds. Since the rotation of the Cp is virtually free, the perpendicular structure was used, resulting in symmetry in the bending about $\theta = 180°$. See Results for definition of θ.

Results

Synthesis of Cp*Ru(X)L Species. Our synthetic work has employed Cp* as one of the bulky ligands, together with either P^{i}Pr$_2$Ph or PCy$_3$ (Cy = cyclohexyl) as the bulky phosphine. These compounds are conveniently accessible from [(Cp*Ru-

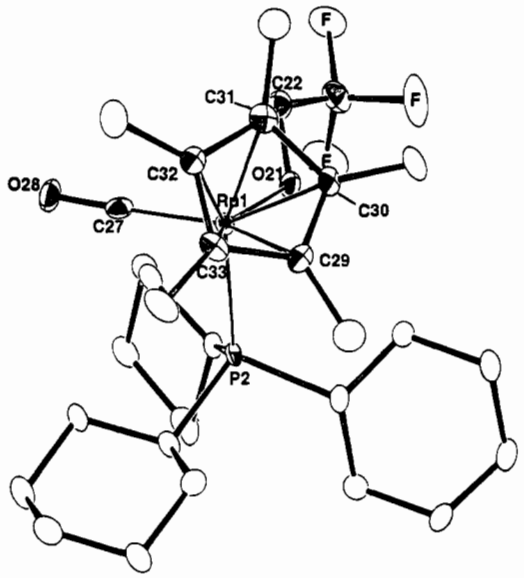

Figure 5. ORTEP drawing of the non-hydrogen atoms of Cp*Ru(PCy$_3$)(CO)(OCH$_2$CF$_3$). Unlabeled ellipses are carbon.

Table 6. Selected Bond Distances (Å) and Angles (deg) for Cp*Ru(PCy$_3$)(CO)(OSiPh$_3$)

Ru(1)−P(4)	2.3861(12)	Si(24)−O(23)	1.582(3)
Ru(1)−O(23)	2.126(3)	Si(24)−C(25)	1.889(5)
Ru(1)−C(2)	1.839(5)	Si(24)−C(31)	1.897(4)
Ru(1)−C(43)	2.238(4)	Si(24)−C(37)	1.896(4)
Ru(1)−C(44)	2.222(4)	O(3)−C(2)	1.161(5)
Ru(1)−C(45)	2.284(4)	Ru−CTR	1.907(4)
Ru(1)−C(46)	2.287(4)	C(43)−C(44)	1.438(6)
Ru(1)−C(47)	2.278(4)	C(43)−C(47)	1.415(6)
P(4)−C(5)	1.859(4)	C(44)−C(45)	1.436(7)
P(4)−C(11)	1.857(4)	C(45)−C(46)	1.432(6)
P(4)−C(17)	1.866(4)	C(46)−C(47)	1.433(7)
P(4)−Ru(1)−O(23)	83.48(8)	C(5)−P(4)−C(17)	102.37(20)
P(4)−Ru(1)−C(2)	90.72(13)	C(11)−P(4)−C(17)	105.50(19)
O(23)−Ru(1)−C(2)	102.88(16)	O(23)−Si(24)−C(25)	114.29(18)
CTR−Ru(1)−C(2)	116.57(18)	O(23)−Si(24)−C(31)	109.80(17)
CTR−Ru(1)−O(23)	120.13(13)	O(23)−Si(24)−C(37)	114.58(17)
CTR−Ru(1)−P(4)	135.03(12)	C(25)−Si(24)−C(31)	109.83(19)
Ru(1)−P(4)−C(5)	117.33(14)	C(25)−Si(24)−C(37)	105.57(19)
Ru(1)−P(4)−C(11)	116.92(14)	C(31)−Si(24)−C(37)	102.01(18)
Ru(1)−P(4)−C(17)	108.72(14)	Ru(1)−O(23)−Si(24)	142.40(18)
C(5)−P(4)−C(11)	104.48(19)	Ru(1)−C(2)−O(3)	167.2(4)

(μ_3-Cl)]$_4$[11] by addition of phosphine, with scission of the chloride bridges. Our attempt to use a still bulkier phosphine (P^{t}Bu$_2$Ph or P(*o*-tolyl)$_3$) returned only unreacted [(Cp*Ru(μ_3-Cl)]$_4$ after 24 h at 25 °C in hexanes. There are thus limits to the steric bulk which will permit phosphine attack on the tetramer. An alternative reactivity is possible for "slender" ligands, in that CO adds to yield the dimer, (Cp*RuCO)$_2$(μ-Cl)$_2$.[14]

Tricyclohexylphosphine has the undesirable feature of possessing so many inequivalent protons that it obscures the 2.30−0.90 ppm region of the ^{1}H NMR spectrum. We therefore turned to P^{i}Pr$_2$Ph, whose phenyl ring we felt would confer good crystallizability on its complexes. As it turns out, this was not true. Most of these derivatives are oils. Because this is a pyramidal PR$_2$R′ group, the pair of R groups serve as diastereotopic reporters of the presence or absence of a mirror plane of symmetry containing the M−P bond. However, since R here is isopropyl, the two methyls in one ^{i}Pr group will never be equivalent (even in the free phosphine). Thus, a mirror-symmetric Cp*Ru(P^{i}Pr$_2$Ph)X molecule will show *two* methyl chemical shifts, and one lacking a mirror plane will show four methyl chemical shifts.

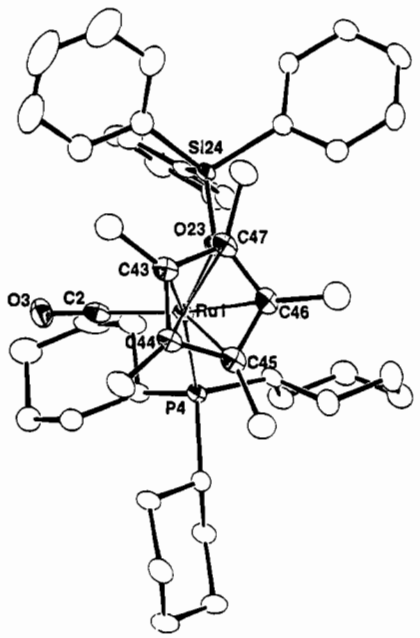

Figure 6. Drawing of the non-hydrogen atoms of Cp*Ru(PCy$_3$)(CO)(OSiPh$_3$) showing selected atom labeling. This view is nearly perpendicular to the Cp* ring plane.

Chloride ion metathesis proceeds efficiently as shown in eq 2 to give derivatives containing a broad range of potential

$$\text{Cp*Ru(Cl)L} + \text{M}^\text{I}\text{X} \rightarrow \text{Cp*Ru(X)L} + \text{M}^\text{I}\text{Cl} \qquad (2)$$

$$\text{M}^\text{I}\text{X} = \text{TlOCH}_2\text{CF}_3,\ \text{KOSiPh}_3,\ \text{KOSiMe}_2\text{Ph},\ \text{LiNHPh}$$

π-donor groups X. These products are all highly air-sensitive purple/violet compounds, each of which shows a singlet ^{31}P{^{1}H} NMR signal, one Cp* methyl proton signal, and, for P = P^{i}Pr$_2$Ph, two methyl chemical shifts and one methine chemical shift. Their air sensitivity foretells of high reactivity and argues against a conventional saturated situation as in RuCl$_2$(PR$_3$)$_4$[15] or Cp*Ru(PMe$_3$)$_2$CH$_3$.[16]

Synthesis and Characterization of [Cp*Ru(OCH$_2$CF$_3$)]$_2$. Our initial synthetic efforts toward an alkoxide species involved metathesis of halide from [Cp*RuCl]$_4$ with TlOCH$_2$CF$_3$. This reaction, carried out for 1 h in pentane, yields a compound characterized by spectroscopic techniques and by X-ray diffraction[17] as the *dimer* [Cp*Ru(OCH$_2$CF$_3$)]$_2$. This demonstrates a considerable distinction in bridging ability between halide and alkoxide ligands.[18] This dimer (Figure 1) displays structural features quite similar to those of [Cp*Ru(OMe)]$_2$.[19,20] The

(13) (a) Ammeter, J. H.; Bürgi, H.-B.; Thibeault, J. C.; Hoffmann, R. *J. Am. Chem. Soc.* **1978**, *100*, 3686. (b) Thorn, D. L.; Hoffmann, R. *Inorg. Chem.* **1978**, *17*, 126.

(14) Kölle, U.; Kang, B.-S.; Englert, U. *J. Organomet. Chem.* **1991**, *420*, 227. Kölle, U.; Ruether, T.; Klaui, W. *J. Organomet. Chem.* **1992**, *426*, 99. Kölle, U.; Hörnig, A.; Englert, U. *J. Organomet. Chem.* **1992**, *438*, 309. Kölle, U.; Kang, B.-S.; Thewalt, U. *Organometallics* **1992**, *11*, 2893.

(15) Meakin, P.; Muetterties, E. L.; Jesson, J. P. *J. Am. Chem. Soc.* **1973**, *95*, 75.

(16) Bryndza, H. E.; Fong, L. K.; Paciello, R.; Tam, W.; Bercaw, J. E. *J. Am. Chem. Soc.* **1987**, *109*, 1444.

(17) Bond lengths and angles are so similar to those of [Cp*RuOMe]$_2$ that we have deposited our structural details on the OCH$_2$CF$_3$ analog as supplementary material.

(18) This point has been examined by: Hörnig, A.; Englert, U.; Kölle, U. *J. Organomet. Chem.* **1993**, *453*, 255.

(19) Loren, S. D.; Campion, B. K.; Heyn, R. H.; Tilley, T. D.; Bursten, B. E.; Luth, K. W. *J. Am. Chem. Soc.* **1989**, *111*, 4712. Kölle, U.; Kossakowski, J. *J. Chem. Soc., Chem. Commun.* **1988**, 549.

structure of $[Cp^*Ru(OCH_2CF_3)]_2$ in the solid state is a dimer with a crystallographic mirror plane containing the two metals and the two Cp* ring midpoints. The Cp* rings on the two ends of the molecule are mutually staggered (minimizing end-to-end repulsions between the methyl groups), and the central Ru_2O_2 core is nonplanar (i.e., puckered). Each C_5 ring is essentially orthogonal (90.3 and 95.9°) to the respective RuO_2 plane. The oxygen atoms are pyramidal (not planar); the sum of angles around oxygen is 339.9(4)°. The Ru−Ru distance (3.026 Å) is considered nonbonding.[19] The two independent Ru−O distances differ by less than 3σ (0.012 Å). All distances and angles are within 10 esd's of the corresponding values in $[Cp^*RuOMe]_2$. This dimer reacts with both P^iPr_2Ph and PCy_3 (1 P/Ru) to furnish alternative syntheses of $Cp^*RuL(OCH_2CF_3)$.

Structural Studies of Cp*Ru(L)X Species. A few general comments pertain to the structures of monomers reported here. No two compounds are crystallographically isomorphous. Cp* ring C−C distances vary insignificantly both within one compound and between compounds. Ru−C(Cp*) distances vary less than 0.05 Å and warrant no special comment.

(a) $Cp^*Ru(P^iPr_2Ph)I$. This two-legged piano stool has ruthenium lying within 0.003 Å of the CTR−P−I plane where CTR is the center of the Cp* ring (Figure 2). This plane is perpendicular (90.1°) to the mean plane of the five Cp* ring carbons. The C−C distances in the C_5 ring differ by less than 4 esd's, and the Ru−C distances differ by less than 7σ (0.042 Å). The rotational conformation adopted by the $Ru(P^iPr_2Ph)$ unit places the phenyl ring *anti* to the iodide and the ^{i}Pr groups *anti* to the Cp* ring. The Ru−I bond length, 2.6642(5) Å, is statistically significantly shorter than that in $(C_5H_4(neomenthyl))Ru(PPh_3)I(CO)$, at 2.708(1) Å.[21] This could be attributed to I → Ru π donation or to the lower coordination number in $Cp^*Ru(PCy_3)I$. This question will be addressed below by extended Hückel calculations.

(b) $Cp^*Ru(PCy_3)(OCH_2CF_3)$. The X-ray diffraction study shows (Figure 3) that $Cp^*Ru(PCy_3)(OCH_2CF_3)$ adopts a two-legged piano-stool structure. The angle between the Ru/P/O plane and that of the five Cp* ring carbons is 91.6°. The Cp* ring shows conventional η^5-binding, and the rotational conformations about the cyclohexyl rings are staggered with respect to the Ru−O bond. This directs one cyclohexyl ring toward the Cp* group, but a space-filling drawing shows that this does not produce excessive steric hindrance. All cyclohexyl rings place phosphorus in an equatorial position on a chair form. The alkoxide C−O bond lies *anti* to the phosphine, and the CF_3 group is then directed away from the Cp* group. The Ru−P bond length, 2.418(4) Å, while long, is insignificantly different from that (2.395(2) Å) in $Cp^*Ru(P^iPr_3)Cl$[5] and merely reflects the steric bulk of both the Cp* and the PCy_3 groups. The P−Ru−O angle, 81.6(3)°, is significantly smaller than the P−Ru−Cl angle, 91.5(1)°, in $Cp^*Ru(P^iPr_3)Cl$.

The Ru−O distance, 1.992(10) Å, is short, in comparison to the value (2.153(6) Å) in *cis*-$RuH(O-aryl)(PMe_3)_4$.[22] The Ru−O−C angle, 124.6(9)°, is larger than the sp^2 angle but is considerably smaller than the angle in early-transition-metal alkoxides and even smaller than the 138.0(11)° value in $IrH_2(OCH_2CF_3)(PCy_3)_2$.[1]

Of importance is the fact that Ru−O and CH_2 lie in the idealized molecular mirror plane. This orients that oxygen lone pair which lies perpendicular to the $RuOCH_2$ plane for maximum π overlap with a ruthenium d_π acceptor orbital (see below).

(c) $Cp^*Ru(PCy_3)(OSiPh_3)$. This molecule (Figure 4) adopts the two-legged piano-stool structure. The Ru/P/O plane makes an angle of 91.9° with the plane of the five Cp* ring carbons. Ruthenium is coplanar with P, O, and the Cp* ring center to within 0.007 Å. Carbon−carbon distances within the Cp* ring are identical to within 6 esd's. However, Ru−C distances vary by 18σ, but not in a fashion which reflects the mirror symmetry of the Ru−P−O−Si unit. The Ru−C(4) distance is significantly shorter than the other four. This asymmetry may thus be due not to electronic effects of the donor atom but rather to the steric influence of ligand substituents. One cyclohexyl ring stacks face-to-face with one phenyl ring; the angle Ru−P−C to that cyclohexyl is 10° smaller than those to the other two cyclohexyl *ipso*-carbons. The (modest) deviation of silicon from the RuPO (mirror) plane occurs to move the $SiPh_3$ group away from the PCy_3 group. This conformation maximizes overlap of the higher energy oxygen lone pair (see below) with ruthenium. The Ru−O−Si angle (153.49(11)°) is much larger than the Ru−O−C angle (124.6(9)°) in $Cp^*Ru(PCy_3)(OCH_2CF_3)$.

Electronic Structure of d^6 $CpML_2$. We deal here first with the question of why CpRuLX species are planar about the metal. Why should the unsaturated Ru(II) center in CpRuLX (L = PR_3; X = Cl, I, OCH_2CF_3, $OSiPh_3$) choose not to have an empty coordination site with a sterochemically-active empty orbital like other d^6 pentacoordinated fragments such as $Cr(CO)_5$[23a] or $RuCl_2(PPh_3)_3$?[23b] In 1977, Hofmann[24] analyzed the orbitals of the related unsaturated species $CpMn(CO)_2$ and demonstrated that a pyramidal structure was indeed preferred, leaving an empty coordination site at the manganese. An *ab initio* calculation for a d^6 Cp−metallacyclobutene has also indicated the preference for a pyramidal structure.[25] These analyses are in good agreement with the retention of stereochemistry by the intermediate $CpRe(PR_3)(NO)^+$, although this species was not isolated.[26,27]

We can explain the apparent paradox of CpRuLX structure using a recently-published analysis of the variation in the structure of ML_5 d^6 complexes with different ligand types.[28] As summarized above, in the presence of π-acceptor ligands or with more than one π-donor ligand, ML_5 d^6 complexes are known to have a square-pyramidal structure. Thus, when Cp occupies three facial sites of a square pyramid, the metal is predicted to be pyramidal, **C**, e.g., $CpMn(CO)_2$. In contrast,

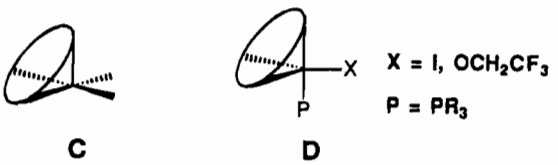

C **D**

ML_4X d^6, where X is a π-donor ligand, is predicted to adopt a distorted trigonal bipyramidal structure with an M−X multiple bond and no stereochemically-active empty orbital. In the Ru-

(20) Kölle, U.; Kossakowski, J.; Boese, R. *J. Organomet. Chem.* **1989**, *378*, 449. For a thiolate analog, see: Takahashi, A.; Mizobe, Y.; Matsuzaka, H.; Dev, S.; Hidai, M. *J. Organomet. Chem.* **1993**, *456*, 243. Kölle, U.; Rietmann, C.; Englert, U. *J. Organomet. Chem.* **1992**, *423*, C20.
(21) Cesarotti, E.; Chiesa, A.; Ciani, G. F.; Sironi, A.; Vefghi, R.; White, C. *J. Chem. Soc., Dalton Trans.* **1984**, 653.
(22) Osakada, K.; Ohshiro, K.; Yamamoto, A. *Organometallics* **1991**, *10*, 404.
(23) (a) For a review article on the structures of $M(CO)_5$ fragments, see: Poliakoff, M.; Weitz, E. *Adv. Organomet. Chem.* **1986**, *25*, 277. (b) La Placa, S. J.; Ibers, J. A. *Inorg. Chem.* **1965**, *4*, 778.
(24) Hofmann, P. *Angew. Chem., Int. Ed. Engl.* **1977**, *16*, 536.
(25) Wakatsuki, Y.; Miya, S.-Y.; Ikuta, S.; Yamazaki, H. *J. Chem. Soc., Chem. Commun.* **1985**, 35.
(26) A recent report concludes that Cp*Ru(acac) has a pyramidal Ru center. This has subsequently shown to be an interpretive error. See: Andersen, R. A.; Hollander, F. *Angew. Chem., Int. Ed. Engl.* **1993**, *32*, 1294.

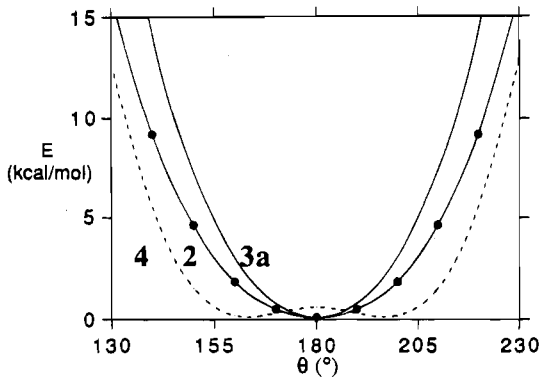

Figure 7. Total energy curves for $CpRuH_2^-$, **2** (unbroken line with the values marked), $CpRu(PH_3)I$, **3a** (plain unbroken line), and $CpRu(CO)_2^+$, **4** (dashed line) for bending of the L−Ru−X plane by θ from the planar structure ($\theta = 180°$) (see text).

(II) complex described above, the Cp replaces three *fac* ligands and the planar structure is observed, **D**. Although these conclusions can be deduced from previous work based on the relationship between the structure of CpRuLX and a distorted trigonal bipyramid, a theoretical study of the complex, explicitly incorporating Cp, gives further insight.

Extended Hückel (EHT) calculations were used to examine the stability of various $CpRuL_2$ complexes when the RuL_2 moiety is bent from a planar structure (**D**) toward a pyramidal structure (**C**). The angle between the plane L−Ru−X and the Ru−Cp vector is defined as θ, **E**(thus in the case of **D**, θ =

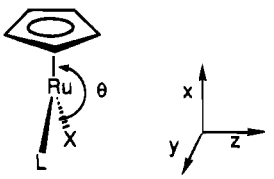

E

180°, whereas for **C**, $\theta \neq 180°$). The structure of $CpMn(CO)_2$, **1**, was previously found to have a bent structure with $\theta = 160°$.[24] Here, we investigate the influence of the ligand orbitals on the complex geometries by analyzing the structure of four model complexes: $CpRuH_2^-$, **2**, $CpRu(PH_3)I$, **3a**, $CpRu(PH_3)(OH)$, **3b**, and $CpRu(CO)_2^+$, **4**.

As shown in Figure 7, the metal is calculated to remain planar for **2** and **3a** (and **3b**, which is not shown in Figure 7) but there is a weak preference for a bent structure ($\theta = 160°$) for **4**, which is in agreement with the previous calculation for **1**.[24] The calculations also show that there is a stronger preference for **3a** and **3b** to be planar compared to **2**. This means that the presence of a π-donor ligand increases the preference for a planar structure over a σ-donor ligand. The calculations also demonstrate that there is no rotational preference for the Cp ring with respect to the ML_2 fragment for any value of θ.[29]

The variation of the sum of the energies of the three occupied d orbitals (1a″, a′($x^2 - y^2$), and a′(z^2), in C_s symmetry, where the mirror plane bisects the ML_2 bonds)[30] reflects the change in the total energy as a function of θ, and thus we can focus on these three orbitals. Figure 8 shows the Walsh diagrams for these three MO's as well as for the LUMO (3a′, which is mainly *xz*) of each complex[31] **2**, **3a** (identical for **3b**, which is not shown), and **4**. Drawings of the metal component of these orbitals (excluding any ligand contribution) are given in **F**. For

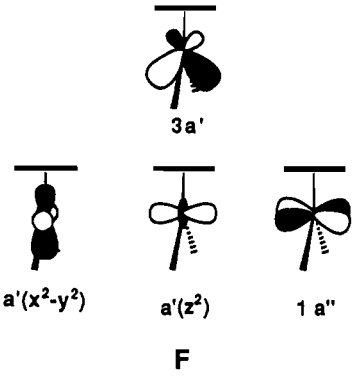

F

each of the systems, **2**, **3a**, and **4**, the a′($x^2 - y^2$) energy is essentially invariant with θ and will not be discussed further. The 1a″ orbital is destabilized as θ departs from 180° because of increasing antibonding interaction with the ligand σ-donor orbitals. Only a′(z^2) is stabilized upon bending due to mixing with the LUMO (3a′) which is thus destabilized. The competition between the destabilization of 1a″ and the stabilization of a′(z^2) determines the ground state geometry (pyramidal *vs* planar at ruthenium). If the energy difference between a′(z^2) and the LUMO is small, there is strong mixing, the stabilization of a′(z^2) is large, and the molecule prefers a pyramidal structure. This is the case for **4** where the LUMO is the in-phase combination of the metal *xz* and the π^*_{CO} orbitals and is low in energy. In **2**, with pure σ-donor ligands, the LUMO is higher in energy because it has no ligand π^* stabilization. The LUMO−a′(z^2) energy difference is now much larger, and the stabilization of a′(z^2) is not sufficiently large to compensate the destabilization of 1a″. Thus, molecule **2** favors a planar structure. Finally, in the presence of a π-donor ligand, as is the case in **3a** (and **3b**), the LUMO−a′(z^2) energy difference is even larger because the 3a′ metal orbital is destabilized by the iodide p_z lone pair. Thus very little stabilization of a′(z^2) is observed upon bending and the destabilization of 1a″ now dominates the behavior of the complex, leading to a net preference (stronger than in **2**) for a planar structure as shown in Figure 7.

The destabilization of the 3a′ orbital by the p_z lone pair of iodine is mirrored in the occurrence of a M−X partial π bond which is to be found in the bonding combination of 3a′ and the iodide p_z lone pair:

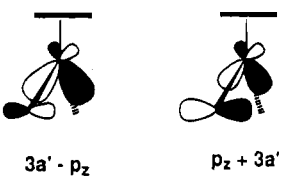

The planar geometry permits maximal overlap between the p_z lone pair of X with the metal 3a′ LUMO. In the case of the OCH_2CF_3 group, the higher-lying (i.e., higher energy) oxygen pure p_z lone pair is a better π donor than the σ one. As a

(27) Fernandez, J. M.; Emerson, K.; Larsen, R. H.; Gladysz, J. A. *J. Am. Chem. Soc.* **1986**, *108*, 8268.
(28) (a) Rachidi, I. E.-I.; Eisenstein, O.; Jean, Y. *New J. Chem.* **1991**, *14*, 671. (b) Riehl, J.-F.; Jean, Y.; Eisenstein, O.; Pélissier, M. *Organometallics* **1992**, *11*, 729.
(29) Albright, T. A.; Hofmann, P.; Hoffmann, R. *J. Am. Chem. Soc.* **1977**, *99*, 7546.
(30) Note that the notation 1a′ and 2a′ for a′($x^2 - y^2$) and a′(z^2) cannot be used here because of the reversal of the ordering of these two orbitals in **4** where a′($x^2 - y^2$) is stabilized by π^*_{CO} and is lower in energy than a′(z^2).
(31) The highest d orbital (mostly *xy* in our set of coordinates), which is antibonding with respect to Cp and the two ligands, is not shown since it does not play any role.

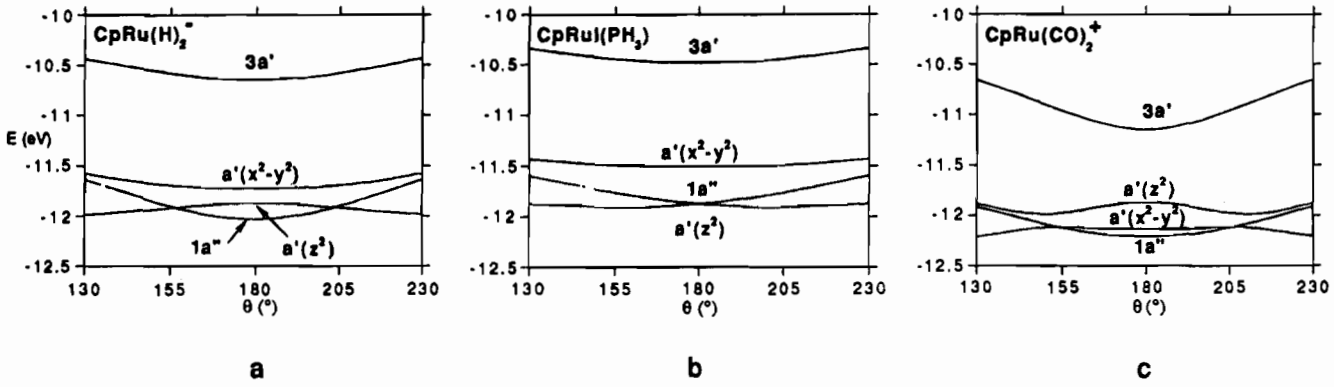

Figure 8. Walsh diagrams for (a) $CpRuH_2^-$, **2**, (b) $CpRu(PH_3)I$, **3a**, and (c) $CpRu(CO)_2^+$, **4**, for bending of the L−Ru−X plane by ν from the planar structure ($\theta = 180°$). Each diagram shows the LUMO (3a′) and the three highest occupied orbitals (1a″, a′($x^2 - y^2$), and a′(z^2)).

Scheme 1. Ranking of ν_{CO} Values (cm^{-1}) of Group X in $Cp^*Ru(P^iPr_2Ph)(CO)X$

I (1930) > Br (1928) > Cl (1925) » OCH_2CF_3 (1914) > $OSiPh_3$ (1906)

> NHPh (1904) > $OSiMe_2Ph$ (1903)

consequence, the O−C bond is coplanar with the P−Ru−O plane for best overlap and energy match with the metal-accepting orbital. A similar effect[28] operates in $Ir(H)_2(OCH_2CF_3)(PCy_3)_2$.[1]

Figure 8 also shows that the LUMO remains low in energy (in spite of the implied X−Ru π donation which would tend to give a large HOMO/LUMO gap characteristic of an 18-valence electron complex) which is responsible for the blue/violet color of the Cp*RuLX compounds (this color is lost in the CO adducts reported below). This same LUMO will initiate adduct formation.

CO Adducts. All of the Cp*RuLX molecules rapidly add CO at 1 atm and 25 °C, with vivid color change from blue or purple to orange/yellow. We have worked up these rapid reactions within 2 min of exposure to CO to avoid possible displacement of bulky phosphine by excess CO (with formation of $[Cp^*Ru(CO)(\mu\text{-}X)]_2$).[14] The resulting Cp*RuL(CO)X products show all the NMR spectroscopic features characteristic of a chiral metal center. In particular, two ^{i}Pr methine and four ^{i}Pr methyl chemical shifts are resolved. The OCH_2CF_3 protons are diastereotopic, as are the $OSiMe_2Ph$ methyl protons, and thus each shows two chemical shifts; before carbonyl addition, these nuclei each showed only one chemical shift. The doublet ($J_{CP} \approx 20$ Hz) in the $^{13}C\{^1H\}$ NMR spectra of 99% enriched $Cp^*Ru(PR_3)X(^{13}CO)$ confirms that neither PR_3 nor CO undergoes dissociation on the NMR time scale.

Several points about numerical chemical shifts warrant mention. Isopropyl methyl proton chemical shifts move 0.4−0.7 ppm upfield on CO adduct formation, and ^{i}Pr methine proton chemical shifts are even more sensitive (upfield shifts as large as 1.2 ppm). Such shifts are far larger than those of any other proton in the molecule. Moreover, the methylene protons of OCH_2CF_3 appear to reflect changes in π donation since they change (upfield) ~1 ppm on CO binding.

Given these substantial chemical shift effects, it became of interest to look for analogous changes in silicon of the siloxides by ^{29}Si NMR spectroscopy. Samples of $Cp^*Ru(PCy_3)(OSiPh_3)$ and $Cp^*Ru(PCy_3)(CO)(OSiPh_3)$ (whose purity was confirmed by their ^{31}P NMR spectra) were found to have ^{29}Si chemical shifts of −22.2 and −22.4 ppm at 25 °C in 80:20 toluene/C_6D_6. Any change in the electronic environment at silicon is thus not well reflected in the silicon chemical shift, perhaps because of altered Si/O bonding as the Ru/O bond is altered.

Consistent with the idea that there is a suppression of ^{29}Si chemical shift change by altered O/Si bonding is the fact that the ^{13}C chemical shift of the CH_2 carbon in OCH_2CF_3 changes by over 20 ppm on CO adduct formation. For comparison, the CF_3 and CH_3 carbon chemical shifts change by less than 1.5 ppm on adduct formation.

Scheme 1 summarizes the stretching frequencies of the carbonyl ligand as the group X is varied. This shows all the alkoxide and amide ligands to be better donors than any of the halides surveyed and also the expected higher siloxide donor power as phenyl groups are replaced by methyl. Similar trends were observed in $Ru^{II}XH(CO)(PR_3)_2$.[2] These data (see Experimental Section) also show that PCy_3 is a better donor than P^iPr_2Ph; ν_{CO} drops 4−5 cm^{-1} on going to PCy_3.

Ethylene Binding. We have employed ethylene as a weaker (hence more discriminating) probe of $Cp^*Ru(PR_3)X$ Lewis acidity than CO. Ethylene also represents a substrate which is more bulky and thus may feel more strongly the steric constraints of Cp* and of bulky phosphines but is also a weaker π-acid than CO.

When toluene-d_8 solutions of $Cp^*Ru(P^iPr_2Ph)X$ (X = OR_f, Cl, I, where $R_f = CH_2CF_3$) are reacted in an NMR tube with equimolar $(^{13}C)_2H_4$ at 25 °C, the degree of binding of ethylene is dependent on the identity of X. Virtually no adduct formation is observed (^{13}C, ^{31}P NMR) for the alkoxide complex at this temperature. However, 80% of the chloride and all of the iodide form a 1:1 adduct under these conditions. Ethylene binding thus correlates with ν_{CO} trends (Scheme 1), provided that we accept that low ν_{CO} means X → Ru π donation which competes with adduct formation. At −60 °C, all three species completely bind ethylene, and ethylene rotation has been halted (two carbon resonances are seen for bound ethylene).[32]

Other Reactions. The limits of Lewis acidity of $Cp^*Ru(PR_3)X$ species can be best tested by using very weak nucleophiles. Chlorobenzene is only weakly basic, yet it will bind to "$CpRe(NO)(PPh_3)^+$".[33] We find no evidence (^{1}H, ^{31}P NMR spectra) for binding of PhCl, even with 3 equiv, to $Cp^*Ru(PR_3)(OR_f)$ in toluene-d_8 in the temperature range +25 to −60 °C.

On the other hand, methyl iodide reacts with $Cp^*Ru(P^iPr_2Ph)(OR_f)$ in less than 1 h in pentane at 25 °C to deposit (at −20 °C) blue crystals of $Cp^*Ru(P^iPr_2Ph)(I)$. Proton NMR revealed the concurrent production of $MeOR_f$. Since we anticipate reduced nucleophilicity (due to O → Ru π donation)

(32) For a study of ethylene reactivity toward $[Cp^*RuOMe]_2$, see: Kölle, U.; Kang, B.-S.; Spaniol, T. P.; Englert, U. *Organometallics* **1992**, *11*, 249.

(33) Winter, C. H.; Veal, W. R.; Garner, C. M.; Arif, A. M.; Gladysz, J. A. *J. Am. Chem. Soc.* **1989**, *111*, 4766.

in the ground state of Cp*Ru(P^{i}Pr$_2$Ph)(OR$_f$), this reaction was anticipated to occur via intermediate **G**. However, a 6:1 ratio

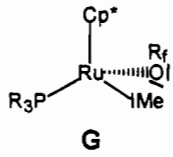

G

of MeI and Cp*Ru(P^{i}Pr$_2$Ph)(OR$_f$) in toluene-d_8 showed no change in ^{31}P or ^{1}H NMR signals of the reagent complex or of MeI over the temperature range −35 to −80 °C. In a similar manner, Cp*Ru(P^{i}Pr$_2$Ph)(OR$_f$) reacts with Me$_3$SiCl within 10 min at 25 °C in pentane to give Cp*Ru(P^{i}Pr$_2$Ph)(Cl).[34]

Structures of CO Adducts. A few general observations are appropriate. Average Ru−C(Cp*) distances lengthen by 0.12 Å upon addition of CO, while the Ru−P distances decrease by 0.01 Å (X = OSiPh$_3$) and 0.042 Å (X = OCH$_2$CF$_3$). Against this background, *the changes in the Ru−X distances and the Ru−O−E angles are the largest consequences of binding CO.*

(a) Cp*Ru(PCy$_3$)(CO)(OCH$_2$CF$_3$). This three-legged piano stool (Figure 5) has one cyclohexyl group interleaving the Ru−O and Ru−CO vectors, and the CH$_2$CF$_3$ group is still directed away from the PCy$_3$ group. The Ru−C(Cp*) distances vary greatly (0.114 Å or 19σ), with the two longest values *trans* to CO. The Ru−O distance is lengthened 0.1 Å by addition of CO, and the Ru−O−C angle is decreased by only 1.7° (to 122.9(3)°). Two of the angles between the legs of the piano stool deviate greatly from 90°: P−Ru−O = 78.78(9)° and OC−Ru−O = 101.08(16)°. This is the same pattern seen for Cp*Ru(PCy$_3$)(CO)(OSiPh$_3$). Remarkably, the Ru−P distance *decreases* by 0.042(4) Å (to 2.376(1) Å) upon coordination of CO.

(b) Cp*Ru(PCy$_3$)(CO)(OSiPh$_3$). This three-legged piano stool (Figure 6) is formed by CO addition with minimal (<2°) reduction in ∠O−Ru−P but with a significant (10°) reduction in ∠Ru−O−Si. The former suggests that, even in Cp*Ru(PCy$_3$)(OSiPh$_3$), the P−Ru−O angle is near its minimum value due to repulsion between bulky groups. The latter bend occurs to increase the separation between the bulky PCy$_3$ and SiPh$_3$ groups. Again, the ∠Ru−P−C$_{ipso}$ of the cyclohexyl group most directed toward the OSiPh$_3$ group is 8° smaller than the other two Ru−P−C angles. The angle O−Ru−CO (102.88°) is quite large,[35] even in comparison to ∠P−Ru−CO (90.72°). This suggests that this large angle is of electronic origin, since the smallest angle (83.5(1)°) involves the bulkier PCy$_3$ and OSiPh$_3$ groups. The three Ru−C (Cp* ring) distances which are roughly *trans* to the Ru−CO bond are longer than the other two by some 0.05 Å (11σ). There is no significant variation in C−C distances within the C$_5$ ring, however.

The increased bending at the siloxide oxygen of this CO adduct is possible since the metal has no low-lying empty orbital which demands π donation. Note also that CO addition relaxes the requirement (in Cp*Ru(PCy$_3$)(OSiPh$_3$)) that the SiPh$_3$ group lie in the P−Ru−O plane.

***β*-Hydrogen Elimination.** The preceding results suggest that the compounds Cp*Ru(PR$_3$)X, while saturated in the ground state, are *operationally* unsaturated by the criterion of facile addition of Lewis base. This naturally raises the question of whether β-hydrogen substituents in group X might readily form Ru−H via this same operational unsaturation (eq 3).[36] We have

$$Cp^*(PR_3)Ru(OCH_2R) \rightarrow Cp^*(PR_3)Ru(H)(OCHR) \quad (3)$$

tested Cp*Ru(P^{i}Pr$_2$Ph)(OCH$_2$CF$_3$) for evidence of β-hydrogen migration. It survives unchanged for 66 h at 65 °C in toluene. After 48 h at 95 °C in toluene, there is 50% loss of reagent to at least *three* phosphorus-containing products. This raises the question of whether the CF$_3$ substituent might be the cause of the stability. It could be argued that the CF$_3$ group makes the carbonyl carbon of the resulting CF$_3$C(O)H so electrophilic that the thermodynamics of addition of Ru−H across the O−CH(CF$_3$) bond are very favorable.[37]

The results of chemical ionization (CH_5^+) mass spectroscopic studies provide supplementary confirmation that the lowest energy thermal transformation of Cp*Ru(PR$_3$)(OR$_f$) compounds (for both P^{i}Pr$_2$Ph and PCy$_3$) is phosphine loss, not β-hydrogen migration: the vapors above samples of Cp*Ru(PR$_3$)(OR$_f$) which were slowly ramped to 400 °C contain mostly the dimer [Cp*Ru(OR$_f$)]$_2$.

We have therefore investigated the reaction of KO^{i}Pr with Cp*Ru(P^{i}Pr$_2$Ph)Cl. This proceeds, in 5 min at 25 °C, to uncharacterized orange-yellow products which show four ^{31}P and four Cp* methyl resonances.[38] No hydrides are evident. The isopropoxide is thus thermolabile and decomposes unselectively, consistent with the functional unsaturation we claim above.

Discussion

The structural data are assembled in Table 7. We will examine these data for evidence that an additional ligand L in Cp*Ru(PR$_3$)(X)L disrupts any π character of the Ru−X bond in Cp*Ru(PR$_3$)X. That is, will the 18-electron rule dictate that the Ru−X bond in Cp*Ru(PR$_3$)(X)L be a pure σ bond? We first need to establish the increase in "inherent size" of Ru (e.g., its single-bond covalent radius) upon increasing the coordination number by 1. In this regard, the Ru−CTR distance increases about 0.1 Å on addition of CO. On the other hand, the Ru−P distances *contract* slightly (0.01−0.04 Å). There seems to be little to conclude beyond the general expectation that the metal single-bond radius must increase slightly. The 0.1 Å Ru−O bond lengthening on binding CO does support the idea that the Cp*Ru(PR$_3$)(OR) class of molecules are stabilized by π donation: there is an Ru/O multiple bond prior to adding CO. These molecules are thus not clearly "unsaturated". The literature provides further evidence for π stabilization of unsaturation for Cp*Ru(PR$_3$)X where X = I[21] and Cl.[5,39] Binding of CO to these molecules causes Ru−X bond lengthening of 0.04 and 0.06 Å, respectively. Both changes are less than those for OR ligands in Table 7. These *trends* in Δ(Ru−X) (although they bear only one significant digit) furnish independent support for the inherently more sensitive trends in X-group donor power derived from ν_{CO} values: I < Cl < OR.

The Ru−O−E angle does undergo a (modest) contraction on adding CO. The lowest "empty" metal d orbital is antisymmetric with respect to the molecular mirror plane of Cp*Ru(PR$_3$)X and is thus potentially π bonding toward X. However,

(34) For the conversion of (Cp*RuOMe)$_2$ to (Cp*RuCl)$_4$ using Me$_3$SiCl, see: Kölle, U.; Kossakowski, J. *J. Organomet. Chem.* **1989**, *362*, 383.

(35) Such deviations from a 90° angle between the legs of CpRe(NO)(PR$_3$)X species are common when X is a strong π donor (e.g., NHPh, OR, and even Cl). See: Dewey, M. A.; Knight, D. A.; Arif, A.; Gladysz, J. A. *Chem. Ber.* **1992**, *125*, 815.

(36) Jia, G.; Lough, A. J.; Morris, R. H. *Organometallics* **1992**, *11*, 161.

(37) RuH$_2$(PPh$_3$)$_4$ reacts with PhC(O)CF$_3$ to give RuH[OCH(CF$_3$)Ph](PPh$_3$)$_3$. See: Hayashi, Y.; Komiya, S.; Yamamoto, T.; Yamamoto, A. *Chem. Lett.* **1984**, 1363.

(38) It has been shown that LiO^{t}Bu will deprotonate the Cp* methyl in Cp*Ru(COD)Cl. See: Kölle, U.; Kang, B.-S.; Thewalt, U. *J. Organomet. Chem.* **1990**, *386*, 267.

(39) For an Ru−Cl distance in the saturated species (menthyl-C$_5$H$_4$)Ru(CO)(PPh$_3$)Cl, see: Cesarotti, E.; Ciani, G.; Siro, A. *J. Organomet. Chem.* **1981**, *216*, 87.

Table 7. Summary of Structural Parameters of Cp*Ru(PR$_3$)(X)L Complexes

X, L	Ru−X, Å	Δ(Ru−X),[b]	Ru−P, Å	∠Ru−O−E,[a] deg	∠P−Ru−X, deg	Ru−CTR,[c] Å
OR$_f$, −	1.992(10)		2.418(4)	124.6(9)	81.6(3)	1.79
OR$_f$, CO	2.090(3)	0.1	2.376(12)	122.9(3)	78.8(1)	1.90
OSiPh$_3$, −	2.028(2)		2.396(1)	153.5(1)	85.0(1)	1.77
OSiPh$_3$, CO	2.126(3)	0.1	2.386(1)	142.4(2)	83.5(1)	1.90

[a] E = C or Si. [b] Δ(Ru−X) = Ru−X bond lengthening by addition of CO. [c] CTR = Cp* ring center.

Scheme 2

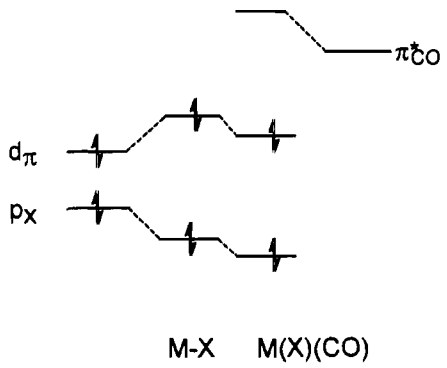

the two lone pairs of the OR group are not degenerate. Instead, one lies in the Ru−O−R plane ($\sigma_{\|}$) and one lies perpendicular to that plane ($p_{\perp}$). The former lies deeper in energy and is

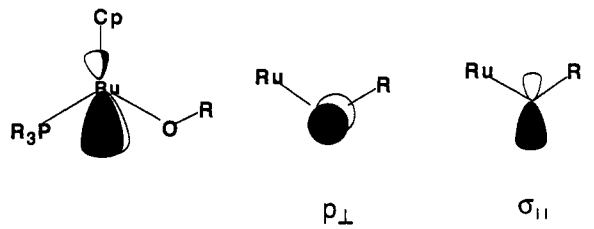

directed somewhat away from Ru, both by virtue of being mixed with the oxygen s orbital. Thus $p_{\perp}$ is better suited for bonding with the metal. Most significantly, formation of *one* Ru/O π bond, involving as it does the pure O(p_{π}) orbital ($p_{\perp}$), should not be improved to first order by an increase in the Ru−O−R angle. Any changes observed when Ru/O π bonding is altered will, in the main, reflect factors *other than* altered π bonding.[40]

We initiated our structural study of pairs of Cp*Ru(PR$_3$)X and Cp*Ru(PR$_3$)LX compounds based on the 18-electron rule: incoming ligand L needs an empty Ru orbital for bonding, so X must play a purely σ-bonding role in the L adduct.[1] This idea is valid if the ligand L carries a purely σ-occupied orbital (e.g., H$^-$). However, we have come to recognize[2] that the π* orbital(s) on our chosen ligand L will stabilize what would ordinarily be a net antibonding interaction (Scheme 2) and thus permit retention of some of the X → Ru π donation present in Cp*Ru(PR$_3$)X itself. Thus, the Ru−X distances we report here for Cp*Ru(PR$_3$)(CO)X represent only *lower limits* to a pure σ Ru−X bond length, and the effect of multiple bonding on Ru−X bond length will thus be greater than indicated by the measured values shown in Table 7.[41] In the extreme case of no π-acceptor neutral ligands to delocalize the metal t_{2g} electrons, the filled/filled repulsion leads to an extremely long Ru−Cl distance (2.51 Å) in Cp*Ru(Me$_2$NC$_2$H$_4$NMe$_2$)Cl.[42] The retention of π bonding in CpM(π-acid)(PR$_3$)X species has been analyzed earlier for Cp*Re(NO)(PR$_3$)X molecules and has been used to understand the rotational conformation about the Re−X bond.[43]

The idea of variable π donation, of course, has its precedents. Variable electron donation has been observed or proposed for a variety of ligands: linear/bent NO, η^5/η^3-Cp, η^3/η^1-allyl, η^2/η^1-acyl, as well as four- and two-electron-donor alkynes and three- and one-electron-donor phosphides. Thiolate ligands, in particular, have a well-developed body of evidence supporting their variable electron donor number.[44]

The Schrock group has already used this principle,[45] with alkoxide groups serving as a tunable parameter for an olefin metathesis catalyst. The presence of halide in a demonstrated ROMP catalyst[46] offers the possibility of activity modification/optimization using the same idea.

In the absence of exceptionally large steric repulsions (such as would exist in RuH$_2$(PPh$_3$)$_4$), an authentic 16-valence-electron configuration[47] is difficult to achieve for 4d^6 or 5d^6 complexes such as those of Ru(II). For example, Lehmkuhl[48] has reported extensive studies of CpRu(PR$_3$)$_2$R complexes, including attack on difficult substrates such as C−H bonds, but these begin with phosphine dissociation and even that can require temperatures as high as 195 °C. This point has been systematized and quantitated:[49] the rate of exchange of free and coordinated phosphines in Cp*Ru(PMe$_3$)$_2$X (by an S$_N$1 mechanism) shows activation energies in the order OH < Cl < CH$_3$ < H. The molecules most reluctant to dissociate phosphine are those where the group X has no lone pair to stabilize the intermediate Cp*Ru(PMe$_3$)X. This same reasoning underlies the *cis*-labilizing effect.[50]

Conclusions

This work has established the viability of the idea that one can use steric encumbrance to protect against double phosphine addition in the conventional synthesis of Cp*RuL$_2$X compounds and thereby create an operationally unsaturated class of molecules Cp*Ru(L)X (L = PCy$_3$ or P^{i}Pr$_2$Ph). A smaller L such as CO permits dimerization by X-bridging and thus loss of unsaturation in the species Cp*$_2$Ru$_2$(CO)$_2$(μ-X)$_2$. Because

(40) Bickford, C. C.; Johnson, T. J.; Davidson, E. R.; Caulton, K. G. *Inorg. Chem.* **1994**, *33*, 1080.

(41) When L′ is a π acid, there is evidence for residual Ru−X multiple bonding in Cp*RuX(L)(L′) molecules for the Ru−Cl distances (Å) from the following L, L′ pairs: PPh$_3$, CO, 2.425(2); (PPh$_3$)$_2$, 2.453(2); (PMe$_3$)$_2$, 2.44. See: Bruce, M. I.; Wang, F. S.; Skelton, B. W.; White, A. H. *J. Chem. Soc., Dalton Trans.* **1981**, 1398. Also, compare to ref 39. The iodide distance (2.664(1) Å) in Cp*Ru(P^{i}Pr$_2$Ph)I should also be compared to the longer value (2.724(1) Å) in CpRu(PPh$_3$)(^{t}-BuNC)I. See: Conroy-Lewis, F. M.; Redhouse, A. D.; Simpson, S. J. *J. Organomet. Chem.* **1989**, *366*, 357.

(42) Wang, M. H.; Englert, U.; Kölle, U. *J. Organomet. Chem.* **1993**, *453*, 127.

(43) Kiel, W. A.; Lin, G.; Constable, A. G.; McCormick, F. B.; Strouse, C. E.; Eisenstein, O.; Gladysz, J. A. *J. Am. Chem. Soc.* **1982**, *104*, 4865. Buhro, W. E.; Zwick, B. D.; Georgiou, S.; Hutchinson, J. P.; Gladysz, J. A. *J. Am. Chem. Soc.* **1988**, *110*, 2427. Quiros Mendez, N.; Arif, A. M.; Gladysz, J. A. *Organometallics* **1991**, *10*, 2199.

(44) Ashby, M. T. *Comments Inorg. Chem.* **1990**, *10*, 297.

(45) Schrock, R. R. *Acc. Chem. Res.* **1989**, *19*, 342; **1990**, *23*, 158.

(46) Nguyen, S. T.; Johnson, L. K.; Grubbs, R. H.; Ziller, J. W. *J. Am. Chem. Soc.* **1992**, *114*, 3974.

(47) By this we mean only σ ligands (e.g., hydride or phosphine) are present. Ligands bearing lone pairs are excluded.

(48) Lehmkuhl, H.; Bellenbaum, M.; Grundke, J.; Mauermann, H.; Krüger, C. *Chem. Ber.* **1988**, *121*, 1719.

(49) Bryndza, H. E.; Domaille, P. J.; Paciello, R. A.; Bercaw, J. E. *Organometallics* **1989**, *8*, 379.

(50) Atwood, J. D.; Brown, T. L. *J. Am. Chem. Soc.* **1976**, *98*, 3160.

Cp^*RuLX is not only operationally unsaturated, but also electron-rich, it is susceptible to oxidative addition: the Ru(II) $\rightleftarrows$ Ru(IV) couple becomes accessible[51] with unusual facility. The first of these features (resistance to dimerization) is shared by $Cp^*_2ZrCl_2$, while the redox option is clearly not possible. Another distinction between the two systems is the high heteroatom affinity of Zr(IV), while $Cp^*Ru(L)X$ compounds permit Ru−X bond scission by reagents as mild as H_2.[4]

A recent review[52] has investigated the earlier perception that bonds from late transition metals to alkoxides are inherently weak and has concluded that they are *not*. Our evidence, reported here, goes beyond that and indicates varying degrees of X → Ru π donation in the species Cp^*RuLX. This conclusion follows from Ru/X bond lengths, from the planar character of the three ligands about ruthenium, and from the rotational conformation about the Ru−O bond when $X = OCH_2CF_3$. An extended Hückel MO analysis reveals how the $Cp^*Ru(PR_3)$ unit is a suitable π acceptor of the lone pair(s) of X. The planar, d^8 electron configuration, upon which much of the earlier review article is based (e.g., $IrX(CO)(PPh_3)_2$ and $PtX_2(PR_3)_2$), is peculiar in *not* having a metal π-acceptor orbital for formation of an effective M−X π bond.[53]

Acknowledgment. This work was supported by the U.S. National Science Foundation (Grant No. CHe-9103915), by the Indiana University Institute for Advanced Study, and by the French CNRS, as well as by an NSF/CNRS grant for U.S./France scientific collaboration. We thank Aesar/Johnson Matthey Corp. for material support and Roger Kuhlman and Paul Coan for assistance with several crucial experiments. The Laboratoire de Chimie Théorique is associated with the CNRS (URA 506) and is a member of the ICMO and IPCM. We also thank the reviewers for thoughtful and insightful comments and observations.

Supplementary Material Available: Listings of crystallographic details, anisotropic thermal parameters, fractional coordinates and isotropic thermal parameters, and bond distances and angles (22 pages). Ordering information is available on any current masthead page.

IC941174I

(51) Campion, B. H.; Heyn, R. H.; Tilley, T. D. *J. Chem. Soc., Chem. Commun.* **1992**, 1201.
(52) Bryndza, H.; Tam, W. *Chem. Rev.* **1988**, *88*, 1163.
(53) Cowan, R. L.; Trogler, W. C. *J. Am. Chem. Soc.* **1989**, *111*, 4750.